Numerical Analysis of a Finite Element Method for an Optimal Control of Bidomain-bath Model

Mostafa Bendahmane, Nagaiah Chamakuri

NUMERICAL ANALYSIS OF A FINITE ELEMENT METHOD FOR AN OPTIMAL CONTROL OF BIDOMAIN-BATH MODEL

MOSTAFA BENDAHMANE* AND NAGAIAH CHAMAKURI †

Abstract. This work is concerned with the study of the convergence analysis for an optimal control of bidomain-bath model by using the finite element scheme. The bidomain-bath model equations describe the cardiac bioelectric activity at the tissue and bath volumes where the control acts at the boundary of the tissue domain. We establish the existence of the finite element scheme, and convergence of the unique weak solution of the direct bidomain-bath model. The convergence proof is based on deriving a series of a priori estimates and using a general L^2-compactness criterion. Moreover, the well-posedness of the adjoint problem and the first order necessary optimality conditions are shown. Comparing to the direct problem, the convergence proof of the adjoint problem is based on using a general L^1-compactness criterion. The numerical tests are demonstrated which achieve the successful cardiac defibrillation by utilizing less total current. Finally, the robustness of the Newton optimization algorithm is presented for different finer mesh geometries.

Key words. Optimal control, Bidomain model, Weak solution, Finite Element Method, First order optimality conditions, Cardiac electrophysiology

1. Introduction. The electrical behavior of the cardiac tissue surrounded by a nonconductive bath is described by a coupled partial and ordinary differential equations which are so called bidomain model equations [17, 22, 24]. The bidomain model equations consist of two parabolic partial differential equations (PDEs) which describe the dynamics of the intra and the extracellular potentials. The PDEs coupled with an ordinary differential equations which model the ionic currents associated with the reaction terms. Furthermore, an additional Poisson problem has to be solved when the cardiac tissue is immersed in a conductive fluid, e.g. tissue bath in an experimental context or a surrounding torso to model in vivo scenarios.

Here, we denote the heart's spatial domain by $\Omega_H \subset \mathbb{R}^3$ which is a bounded open subset, and by Σ_H we denote its piecewise smooth boundary (the heart surface). This is a three-dimensional slice of the myocardium. A distinction is made between the intracellular and the extracellular tissues which are separated by the cardiac cellular membrane. The thorax is modeled by a volume conduction $\Omega_B \subset \mathbb{R}^3$ (which is a bounded open subset). Moreover, Σ_B is the body surface (it is assumed to be smooth). For all $(x,t) \in \Omega_{T,H} := \Omega_H \times (0,T)$, $u_i = u_i(x,t)$, $u_e = u_e(x,t)$ stand for the intracellular and the extracellular potentials respectively, and for all $(x,t) \in \Omega_{T,B} := \Omega_B \times (0,T)$, $u_s(x,t)$ stands for the bathing medium electric potential.

*Institut de Mathématiques de Bordeaux UMR CNRS 5251, Université Victor Segalen Bordeaux 2,F-33076 Bordeaux Cedex and INRIA Centre de Recherche Bordeaux-Sud-Ouest, France. email: mostafa.bendahmane@u-bordeaux.fr

†Radon Institute for Computational and Applied Mathematics (RICAM), Austrian Academy of Sciences, Altenbergerstrabe 69 A-4040 Linz, Austria. email: nagaiah.chamakuri@ricam.oeaw.ac.at

The complete bidomain-bath model equations are given below.

$$
\begin{cases}
\beta c_m \partial_t u - \nabla \cdot (\mathbf{M}_{\rm i}(x)\nabla u_i) + \beta I_{\rm ion}(u,w) = I^i_{\rm app} & (t,x) \in \Omega_{T,H} := (0,T)\times\Omega_H,\\
\beta c_m \partial_t u + \nabla \cdot (\mathbf{M}_{\rm e}(x)\nabla u_e) + \beta I_{\rm ion}(u,w) = I^e_{\rm app} & (t,x) \in \Omega_{T,H},\\
\partial_t w - H(u,w) = 0 & (t,x) \in \Omega_{T,H},\\
-\nabla \cdot (\mathbf{M}_{\rm s}(x)\nabla u_s(t,x)) = 0 & (t,x) \in \Omega_{T,B} := (0,T)\times\Omega_B,\\
\\
(\mathbf{M}_{\rm i}(x)\nabla u_i)\cdot\eta = 0 & (t,x) \in \Sigma_{T,H} := (0,T)\times\Sigma_H,\\
(\mathbf{M}_{\rm e}(x)\nabla u_e)\cdot\eta = \mathcal{I} + (\mathbf{M}_{\rm s}(x)\nabla u_s)\cdot\eta & (t,x) \in \Sigma_1 := \omega\times(0,T) \subset \Sigma_{T,H},\\
(\mathbf{M}_{\rm e}(x)\nabla u_e)\cdot\eta = (\mathbf{M}_{\rm s}(x)\nabla u_s)\cdot\eta & (t,x) \in \Sigma_2 := \Sigma_{T,H}\setminus\Sigma_1,\\
u_e = u_s & (t,x) \in \Sigma_{T,H}\\
(\mathbf{M}_{\rm s}(x)\nabla u_s)\cdot\eta_s = 0 & (t,x) \in \Sigma_{T,B} = \Sigma_B\times(0,T),\\
\\
u(0,x) = u_0(x) & x \in \Omega_H,\\
w(0,x) = w_0(x) & x \in \Omega_H.
\end{cases}
\tag{1.1}
$$

Herein, ω is a part of the heart surface (more precisely the site where the stimulus is applied) and $\mathcal{I}$ is the stimulus which acts as a control on ω. The transmembrane potential is the difference $u = u(x,t) := u_i - u_e$, $\mathbf{M}_{\rm i}(\mathbf{x})$ and $\mathbf{M}_{\rm e}(\mathbf{x})$ are the scaled tensors which represent the intra- and extracellular conductivity tensors of the tissue respectively. The diagonal matrix $\mathbf{M}_{\rm s}$ represents the conductivity tensor of the bathing medium. Let $a_l(\mathbf{x})$, $a_t(\mathbf{x})$ and $a_n(\mathbf{x})$ denotes the fiber, sheet and normal to the sheet directions respectively in the orthonormal basis [18] which depends on the position in the heart. In our computational study, we assumed the rotational isotropy at the tissue structure, i.e. $\sigma^{i,e}_n = \sigma^{i,e}_t$, then the local intracellular conductivity tensor $\mathbf{M}_{\rm i}(\mathbf{x})$ is expressed as

$$
\mathbf{M}_{\rm i}(x) = (\sigma^i_l - \sigma^i_t)\, a_l(\mathbf{x}) a^T_l(\mathbf{x}) + \sigma^i_t\, I\,,
\tag{1.2}
$$

where σ^i_l, σ^i_t denote the measured conductivity coefficients along the corresponding directions and I is the identity matrix. The constant $c_m > 0$ is the capacitance of the membrane and β is the surface-to-volume ratio.

Moreover, $H(u,w)$ and $I_{\rm ion}(u,w)$ are functions which correspond to the fairly simple Mitchell-Shaeffer membrane model for the membrane and ionic currents, see for e.g. [21].

$$
H(u,w) = \frac{w_\infty(u/u_p) - w}{R_{\rm m} c_{\rm m} \eta_\infty(u/u_p)}, \quad I_{\rm ion}(u,w) = \frac{u_p}{R_{\rm m}}\Big(\frac{u}{u_p\eta_2} - \frac{u^2(1-u/u_p)w}{u_p^2\eta_1}\Big),
\tag{1.3}
$$

where the dimensionless functions $\eta_\infty(s)$ and $w_\infty(s)$ are given by $\eta_\infty(s) = \eta_3 + (\eta_4 - \eta_3)\mathcal{H}(s-\eta_5)$ and $w_\infty(s) = \mathcal{H}(s-\eta_5)$, where $\mathcal{H}$ denotes the Heaviside function, $R_{\rm m}$ is the surface resistivity of the membrane, and u_p and $\eta_1,\ldots,\eta_5$ are given parameters. A simpler choice for the membrane kinetics is considered based on the widely known FitzHugh-Nagumo model [15], which is often used to avoid computational difficulties arising from a large number of coupling variables. This model is specified by

$$
H(u,w) = au - bw\,,
\tag{1.4}
$$

$$
I_{\rm ion}(u,w) = -\lambda(w - u(1-u)(u-\theta))\,,
\tag{1.5}
$$

where a, b, λ, θ are given parameters. Moreover, we introduce the condition of compatibility : we suppose that u_e has a zero-mean :

$$
\int_{\Omega_H} u_e(t,x)\,dx = 0 \text{ for all } t \in (0,T).
\tag{1.6}
$$

Note that we can recast the bidomain-bath equation (1.1) to elliptic-parabolic formulations subject to the above boundary and initial conditions, which we use in our numerical computations.

$$
\begin{cases}
\nabla\cdot\big((\mathbf{M}_{\rm e}(x)+\mathbf{M}_{\rm i}(x))\nabla u_e\big)+\nabla\cdot(\mathbf{M}_{\rm i}(x)\nabla u) = I^e_{\rm app}-I^i_{\rm app} & (t,x)\in\Omega_{T,H},\\
\beta c_m\partial_t u-\nabla\cdot(\mathbf{M}_{\rm i}(x)\nabla u)-\nabla\cdot(\mathbf{M}_{\rm i}(x)\nabla u_e)+\beta I_{\rm ion}(u,w)=I^i_{\rm app} & (t,x)\in\Omega_{T,H},\\
\partial_t w-H(u,w)=0 & (t,x)\in\Omega_{T,H},\\
-\nabla\cdot(\mathbf{M}_{\rm s}(x)\nabla u_s)=0 & (t,x)\in\Omega_{T,B}.
\end{cases}
\tag{1.7}
$$

For numerical simulations, the control $\mathcal{I}$ acts at the boundary of the cardiac tissue domain will be decomposed as $\mathcal{I}=I_s(\chi_1-\chi_2)$ for the anode and cathodal stimulation. The χ_1 and χ_2 are characteristic functions at the Γ_1 and Γ_2 boundaries of the tissue domain respectively, see Figure 1 for pictorial representation of different subdomains.

The state equations belong to the system of degenerate reaction-diffusion system. For an isolated heart (with no coupling to a surrounding bath), their existence and uniqueness results were reported for phenomenological models to the physiological models in [16, 7, 25, 5, 20]. On the study of optimization of cardiac defibrillation is investigated by several authors recently. The first work on the theoretical analysis and the controllability of the optimization subject to the FitzHugh-Nagumo model is presented in [8]. Later, systematic analysis of the optimal control of monodomain and bidomain model is presented in [20, 10, 12, 1, 3]. The first attempts to the numerical experiments for optimal control of the monodomain and the bidomain model to predict optimized shock waveforms in 2D [12, 13] and more recently for the optimal control of bidomain-bath model using Mitchell-Shaeffer model in 3D geometries [14, 11]. In those studies the control acts at the boundaries of the bath domain.

In this paper, we study a fully discrete reaction-diffusion system in the context of a finite element for the spatial discretization, whereas the first order backward Euler method is applied for the discretization in time. The present work, devoted to the rigorous study of numerical analysis of such complex bidomain-bath model with more general ionic functions that cover the regularized Mitchell-Shaeffer and Fitzhugh-Nagumo models. Herein, we shall establish the convergence of finite element scheme based on the compactness method. We study an optimal control of the heart activity by the external stimulation which acts at the boundary of the tissue domain. The existence and uniqueness of the adjoint states and the first order necessary optimality conditions are presented. Numerical realization is performed to investigate the qualitative behavior of the model and proposed numerical scheme to solve the optimality system. However, even if the literature related to the numerical methods and models for cardiac electrical activity is quite large, rigorous studies about convergence and stability of numerical solutions are still not well established for general physiological ionic functions.

The structure of the paper is organized as follows : In Section 2 we collect some preliminary material, including relevant notations, conditions imposed on the data of our problem, and a notion of weak solutions to our optimal control problem. Section 3 is devoted to presenting the finite element scheme and stating the main convergence theorem (Theorem 3.1). The proof of Theorem 3.1 is divided into Subsection 3.2 (existence of the scheme), Subsection 3.3 (basic a priori estimates), Subsection 3.4 (L^2-space and time translation estimates), Subsection 3.5 (convergence to a weak solution) and Subsection 3.6 (uniqueness of the weak solution). In Section 4 we introduce the main ingredients of the corresponding optimal control problem, existence of the control (Lemma 4.1), optimality conditions and dual problem. The well-posedness of the dual problem is given in Section 5 (Theorem 5.1). The proof of Theorem 5.1 is divided into Subsection 5.1 (basic a priori estimates) and Subsection 5.2 (L^1-space and time translation estimates, convergence to a weak adjoint solution and uniqueness). The numerical procedure to achieve the successful defibrillation with the optimal control approach and the convergence behavior of the optimization algorithm is presented in Section 7. Finally, in Section 8 we draw some conclusions about the possible extensions to our work.

2. Preliminaries and well-posedness of the direct problem. Before studying our problem, we make some assumptions on data of the bidomain-bath model. We assume $\mathbf{M}_{\rm j}=\mathbf{M}_{\rm j}(x):\Omega_H\to\mathbb{R}$, $j=i,e$, and

$\mathbf{M}_{\rm s} = \mathbf{M}_{\rm s}(x) : \Omega_B \to \mathbb{R}$, are C^1 functions and satisfy

$$\mathbf{M}_{\rm j}(x_1)(\xi_1 - \xi_2)\cdot(\xi_1 - \xi_2) \geq C_M|\xi_1 - \xi_2|^2, \quad \mathbf{M}_{\rm s}(x_2)(\xi_1 - \xi_2)\cdot(\xi_1 - \xi_2) \geq C_M|\xi_1 - \xi_2|^2, \tag{2.1}$$

for a.e. $x_1 \in \Omega_H$ and $x_2 \in \Omega_B$, $\forall \xi_1, \xi_2 \in \mathbb{R}^3$, and with C_M being a positive constant.

We assume that the ionic current $I_{\rm ion}(u, w)$ can be decomposed into $I_{1,\rm ion}(u)$ and $I_{2,\rm ion}(w)$, where $I_{\rm ion}(u, w) = I_{1,\rm ion}(u) + I_{2,\rm ion}(w)$. We assume that $I_{1,\rm ion}, I_{2,\rm ion} : \mathbb{R} \to \mathbb{R}$ and $H : \mathbb{R} \to \mathbb{R}$ are continuous functions, and that there exist $r \in (2, +\infty)$ and constants $\alpha_1, \alpha_2, \alpha_3, \alpha_4, \alpha_5, \alpha_6, \alpha_7, L, l > 0$ such that

$$\begin{aligned}
&\frac{1}{\alpha_1}|u|^r \leq |I_{1,\rm ion}(u)u| \leq \alpha_1\left(|u|^r + 1\right),\ |I_{2,\rm ion}(w)| \leq \alpha_2(|w| + 1),\\
&|H(u, w)| \leq \alpha_3(|u| + |w| + 1),\ \text{and}\ \beta I_{2,\rm ion}(w)u - \alpha_4 H(u, w)w \geq \alpha_5|w|^2,\\
&|H_u(u, w)| + |H_w(u, w)| \leq \alpha_6,\ \text{and}\ |I_{2,{\rm ion},w}(w)| \leq \alpha_7,
\end{aligned} \tag{2.2}$$

$$\tilde{I}_{1,\rm ion} : z \mapsto I_{1,\rm ion}(z) + Lz + l \quad \text{is strictly increasing on } \mathbb{R}. \tag{2.3}$$

Herein, $I_{2,{\rm ion},w}$, H_u and H_w are the derivatives of $I_{2,\rm ion}$ and H with respect to u, w, respectively. Note that, it is rather natural (although not necessary) to require in addition that

$$\forall\, z, s \in \mathbb{R} \quad (\tilde{I}_{1,\rm ion}(z) - \tilde{I}_{1,\rm ion}(s))(z - s) \geq \frac{1}{C}(1 + |z| + |s|)^{r-2}|z - s|^2. \tag{2.4}$$

According to the Mitchell-Shaeffer and Fitzhugh-Nagumo models, the most appropriate value is $r = 4$, which means that the non-linearity $I_{\rm ion}$ is of cubic growth at infinity (recall that in the Mitchell-Shaeffer membrane model, the gating variable w is bounded in L^∞). Assumptions (2.2), (2.3) are automatically satisfied by any cubic polynomial $I_{\rm ion}$ with positive leading coefficient.

Next we will use the following spaces. By $H^m(\Omega)$, we denote the usual Sobolev space of order m. Since the electrical potentials u_i and u_e are defined up to an additive constant, we use the quotient space $\tilde{H}^1(\Omega_H) = H^1(\Omega_H)/\{u \in H^1(\Omega), \quad u \equiv \text{Const}\}$. Given $T > 0$ and $1 \leq p \leq \infty$, $L^p(0, T; \mathbb{R})$ denotes the space of L^p integrable functions from the interval $[0, T]$ into $\mathbb{R}$. The weak solution to the bidomain-bath model (1.1) is defined as follows.

DEFINITION 2.1 (Weak solution). *A weak solution to the system (1.1) is a five tuple function (u_i, u_e, u_s, u, w) such that $u \in L^2(0, T, H^1(\Omega_H)) \cap L^r(\Omega_{T,H})$, $\partial_t u \in L^2(0, T, (H^1(\Omega_H)')) + L^{\frac{r}{r-1}}(\Omega_{T,H})$, $u_i, u_e \in L^2(0, T, \tilde{H}^1(\Omega_H))$, $u_s \in L^2(0, T, H^1(\Omega_B))$, $w \in C([0, T], L^2(\Omega_H))$, and satisfying the following weak formulation*

$$\begin{aligned}
\iint_{\Omega_{T,H}} \beta c_m \partial_t u(t, x)\varphi_i + \iint_{\Omega_{T,H}} \mathbf{M}_{\rm i}(x)\nabla u_i \cdot \nabla\varphi_i + \iint_{\Omega_{T,H}} \beta I_{\rm ion}(u, w)\varphi_i &= \iint_{\Omega_{T,H}} I^i_{\rm app}\varphi_i\\
\iint_{\Omega_{T,H}} \beta c_m \partial_t u(t, x)\varphi_e - \iint_{\Omega_{T,H}} \mathbf{M}_{\rm e}(x)\nabla u_e \cdot \nabla\varphi_e + \iint_{\Omega_{T,B}} \mathbf{M}_{\rm s}(x)\nabla u_s \cdot \nabla\varphi_s&\\
- \iint_{\Sigma_{1,T}} \mathcal{I}\varphi_e + \iint_{\Omega_{T,H}} \beta I_{\rm ion}(u, w)\varphi_e &= \iint_{\Omega_{T,H}} I^e_{\rm app}\varphi_e\\
\iint_{\Omega_{T,H}} \partial_t w(t, x)\varphi_w - \iint_{\Omega_{T,H}} H(u, w)\varphi_w &= 0.
\end{aligned} \tag{2.5}$$

for all $\varphi_i, \varphi_e \in L^2(0, T, H^1(\Omega_H)) \cap L^r(\Omega_{T,H})$, $\varphi_s \in L^2(0, T, H^1(\Omega_B))$ and $\varphi_w \in C([0, T], L^2(\Omega_H))$ with $\varphi_e = \varphi_s$ on $\Sigma_{T,H}$.

3. Finite element scheme and main result. In this section, we present the finite element method approximation of the bidomain-bath model. In the sequel, the existence and uniqueness is provided.

3.1. A finite element method. Let $\mathcal{T}_\nu$ be a regular partition of Ω_ν into tetrahedra K_ν with boundary ∂K_ν and diameter h_{K_ν} where $\nu = H, B$. We define the mesh parameter $h = \max_{K_\nu \in \mathcal{T}_\nu}\{h_{K_\nu}\}$ and the associated finite element space V_ν^h for the approximation of electrical potentials and gating variables (we use piecewise linear finite elements for potentials and gating variables). The involved space is defined as

$$V_\nu^h = \{s \in C^0(\bar{\Omega_\nu}) : \, v|_{K_\nu} \in \mathbb{P}_1(K_\nu) \text{ for all } K_\nu \in \mathcal{T}_\nu\}.$$

The semidiscrete Galerkin finite element formulation reads as follows for the bidomain-bath model equations (1.1). For $t > 0$, find $u_i^h(t), u_e^h(t), u^h(t), w^h(t) \in V_H^h$ and $u_s^h(t) \in V_B^h$ such that (with the standard finite element notation for L^2 scalar products) one has

$$\left\{\begin{array}{l} \beta c_m \dfrac{d}{dt}(u^h(t), \phi^h)_{\Omega_H} + \big(\mathbf{M}_{\rm i}(x)\nabla u_i^h(t), \nabla \phi_i^h\big)_{\Omega_H} \\ \qquad\qquad = \big(I_{\rm app}^i - \beta I_{\rm ion}(u^h(t), w^h(t))\,,\, \phi_i^h\big)_{\Omega_H} \\ \beta c_m \dfrac{d}{dt}(u^h(t), \phi_e^h)_{\Omega_H} - \big(\mathbf{M}_{\rm e}(x)\nabla u_e^h(t), \nabla \phi^h\big)_{\Omega_H} + \big(\mathbf{M}_{\rm s}(x)\nabla u_s^h(t), \nabla \phi_s^h\big)_{\Omega_B} \\ \qquad\qquad - \big(\mathcal{I}^h, \phi_e^h\big)_\omega = \big(I_{\rm app}^e - \beta I_{\rm ion}(u^h(t), w^h(t))\,,\, \phi_e^h\big)_{\Omega_B} \\ \dfrac{d}{dt}(w^h(t), \varphi^h)_{\Omega_H} = (H(u^h(t), w^h(t)), \varphi^h)_{\Omega_H}, \end{array}\right. \tag{3.1}$$

for all $\phi_i^h, \phi_e^h, \varphi^h \in V_H^h$ and $\phi_s^h \in V_B^h$ with $\varphi_e = \varphi_s$ on $\Sigma_{T,H}$. A classical backward Euler integration method is employed for the time discretization of (3.1) with the time step $\Delta t = T/N$. This results in the following fully discrete method: for $t > 0$, find $u_i^h(t), u_e^h(t), u^h(t), w^h(t) \in V_H^h$ and $u_s^h(t) \in V_B^h$ such that

$$\big(u_i^h, u_e^h, u^h, w^h\big)(t,x) = \sum_{n=1}^{N} \big(u_i^{h,n}, u_e^{h,n}, u^{h,n}, w^{h,n}\big)(x) \mathbb{1}_{[(n-1)\Delta t, n\Delta t]}(t),$$

and

$$u_s^h(t,x) = \sum_{n=1}^{N} u_s^{h,n}(x) \mathbb{1}_{[(n-1)\Delta t, n\Delta t]}(t),$$

satisfy the following system

$$\left\{\begin{array}{l} \beta c_m \big(\dfrac{u^{h,n} - u^{h,n-1}}{\Delta t}, \phi_i^h\big)_{\Omega_H} + \big(\mathbf{M}_i(x)\nabla u_i^{h,n}, \nabla \phi_i^h\big)_{\Omega_H} \\ \qquad\qquad = \big(I_{\rm app}^{i,h} - \beta I_{\rm ion}(u^{h,n}, w^{h,n})\,,\, \phi_i^h\big)_{\Omega_H} \\ \beta c_m \big(\dfrac{u^{h,n} - u^{h,n-1}}{\Delta t}, \phi_e^h\big)_{\Omega} - \big(\mathbf{M}_e(x)\nabla u_e^{h,n}, \nabla \phi_e^h\big)_{\Omega_H} + \big(\mathbf{M}_{\rm s}(x)\nabla u_s^{h,n}, \nabla \phi_s^h\big)_{\Omega_B} \\ \qquad\qquad - \big(\mathcal{I}^h, \phi_e^h\big)_\omega = \big(I_{\rm app}^{e,h} - \beta I_{\rm ion}(u^{h,n}, w^{h,n})\,,\, \phi_e^h\big)_{\Omega_H} \\ \big(\dfrac{w^{h,n} - w^{h,n-1}}{\Delta t}, \varphi^h\big)_{\Omega_H} = (H(u^{h,n}, w^{h,n}), \varphi^h)_{\Omega_H}, \end{array}\right. \tag{3.2}$$

for all $\phi_i^h, \phi_e^h, \varphi^h \in V_H^h$, $\phi_s^h \in V_B^h$ and for all $n \in \{1, \ldots, N\}$; the initial condition takes the form (the initial conditions are projected on V_H^h by means of the L^2-Hilbertian projection $\mathbb{P}_{V_H^h}$)

$$(u^{h,0}, w^{h,0}) = (\mathbb{P}_{V_H^h}(u_0), \mathbb{P}_{V_H^h}(w_0)).$$

Here $I_{\rm app}^{i,h}(\cdot)$, $I_{\rm app}^{e,h}(\cdot)$, $\mathcal{I}^h$ are time averages over $[(n-1)\Delta t, n\Delta t]$ of $I_{\rm app}^i$, $I_{\rm app}^e$, $\mathcal{I}$, respectively.

Our first main result for the primal equations is as follows.

THEOREM 3.1. *Assume that* (2.1)-(2.4) *and* (1.6) *hold. Furthermore, assume* $u_0 \in L^2(\Omega_H)$, $w_0 \in L^2(\Omega_H)$, $\mathcal{I} \in L^2(\Sigma_{1,T})$, *and* $I_{\rm app}^j \in L^2(\Omega_{T,H})$ *for* $j = i, e$. *Then the finite element solution* $\mathbf{u}_h = \big(u_i^h, u_e^h, u^h, u_s^h, w^h\big)$, *generated by* (3.2), *converges along a subsequence to* $\mathbf{u} = (u_i, u_e, u, u_s, w)$ *as* $h \to 0$, *where* $\mathbf{u}$ *is a weak solution of* (1.1). *Moreover the weak solution is unique.*

3.2. Existence of the finite element scheme. The existence result for the finite element scheme is given in

PROPOSITION 3.1. *Assume that* (2.1) *and* (2.2) *hold. Then the problem* (3.2) *admits a discrete solution* $\mathbf{u}_h = \big(u_i^h, u_e^h, u^h, u_s^h, w^h\big)$. Let $E_h := V_H^h \times V_H^h \times V_H^h \times V_B^h \times L^2(\Omega_H)$ be a Hilbert space endowed with the obvious norm, let $\mathbf{u}^h = \big(u_i^h, u_e^h, u^h, u_s^h, w^h\big)$ and $\Phi^h = \big(\phi_i^h, \phi_e^h, \phi^h, \phi_s^h, \varphi^h\big) \in E_h$ with $u^h = u_i^h - u_e^h$ and $\phi^h = \phi_i^h - \phi_e^h$.
We now define the mapping $\mathcal{A} : E_h \to E_h$ by

$$
\begin{aligned}
[\mathcal{A}(\mathbf{u}^{h,n}), \Phi^h] =& \beta c_m \left(\frac{u^{h,n} - u^{h,n-1}}{\Delta t}, \phi_i^h \right)_{\Omega_H} + \big(\mathbf{M}_i(x) \nabla u_i^{h,n}, \nabla \phi_i^h\big)_{\Omega_H} - \big(I_{\text{app}}^{i,n,h} - \beta I_{\text{ion}}(u^{h,n}, w^{h,n})\,,\, \phi_i^h\big)_{\Omega_H} \\
&+ \beta c_m \left(\frac{u^{h,n} - u^{h,n-1}}{\Delta t}, \phi_e^h \right)_{\Omega} - \big(\mathbf{M}_e(x) \nabla v_e^{h,n}, \nabla \phi_e^h\big)_{\Omega_H} - \big(I_{\text{app}}^{e,n,h} - \beta I_{\text{ion}}(u^{h,n}, w^{h,n})\,,\, \phi_e^h\big)_{\Omega_H} \\
&+ \big(\mathbf{M}_{\text{s}}(x) \nabla u_s^{h,n}, \nabla \phi_s^h\big)_{\Omega_B} - \big(\mathcal{I}^h, \phi_e^h\big)_{\omega} \\
&+ \left(\frac{w^{h,n} - w^{h,n-1}}{\Delta t}, \alpha_4 \varphi^h \right)_{\Omega_H} - (H(u^{h,n}, w^{h,n}), \alpha_4 \varphi^h)_{\Omega_H},
\end{aligned}
$$

for all $\Phi^h \in E_h$ (recall that α_4 is defined in (2.2)). Note that it is easy to obtain the following bounds from the discrete Hölder inequality.

$$
[\mathcal{A}(\mathbf{u}^{h,n}), \Phi^h] \le C \left\|\mathbf{u}^h\right\|_{E_h} \left\|\Phi^h\right\|_{E_h},
$$

for all $\mathbf{u}^h$ and Φ^h in E_h. This implies that $\mathcal{A}$ is continuous. Our goal now is to show that

$$
[\mathcal{A}(\mathbf{u}_h^n), \mathbf{u}_h^n] > 0 \quad \text{for } \|\mathbf{u}_h^n\|_{E_h} = r > 0, \tag{3.3}
$$

for a sufficiently large r. We observe that

$$
\begin{aligned}
[\mathcal{A}(\mathbf{u}_h^n), \mathbf{u}_h^n] \ge& \frac{\beta c_m}{\Delta t} \left\|u^{h,n}\right\|_{L^2(\Omega_H)}^2 + \frac{\alpha_4}{\Delta t} \left\|w^{h,n}\right\|_{L^2(\Omega_H)}^2 - \frac{\beta c_m}{4\Delta t} \|u_h^n\|_{L^2(\Omega_H)}^2 - \frac{\alpha_4}{2\Delta t} \|w_h^n\|_{L^2(\Omega_H)}^2 \\
&- C(\beta, c_m, \Delta t) \left\|u^{h,n-1}\right\|_{L^2(\Omega_H)}^2 - C(\alpha_4, \Delta t) \left\|w^{h,n-1}\right\|_{L^2(\Omega_H)}^2 \\
&+ \sum_{j=i,e} \big(\mathbf{M}_{\text{j}}(x) \nabla u_j^{h,n}, \nabla u_j^{h,n}\big)_{\Omega_H} + \big(\mathbf{M}_{\text{s}}(x) \nabla u_s^{h,n}, \nabla u_s^{h,n}\big)_{\Omega_B} - \big(\mathcal{I}^h, u_e^h\big)_{\omega} \\
&- \big(I_{\text{app}}^{i,n,h}\,,\, u_i^{h,n}\big)_{\Omega_H} + \big(I_{\text{app}}^{e,n,h}\,,\, u_e^{h,n}\big)_{\Omega_H} + \big(\beta \tilde{I}_{1,\text{ion}}(u^{h,n})\,,\, u^{h,n}\big)_{\Omega_H} \\
&- \beta \big(L\, u^{h,n} + l\,,\, u^{h,n}\big)_{\Omega_H} + \big(\beta I_{2,\text{ion}}(w^{h,n})\,,\, u^{h,n}\big)_{\Omega_H} - (\alpha_4 H(u^{h,n}, w^{h,n}), w^{h,n})_{\Omega_H}.
\end{aligned} \tag{3.4}
$$

Observe that from the trace embedding theorem, Young and Poincare inequalities, and the compatibility condition (1.6), we get

$$
\begin{aligned}
\big(I_{\text{app}}^{i,n,h}\,,\, u_i^{h,n}\big)_{\Omega_H} - \big(I_{\text{app}}^{e,n,h}\,,\, u_e^{h,n}\big)_{\Omega_H} + \big(\mathcal{I}^h, u_e^h\big)_{\omega} &= \big(I_{\text{app}}^{i,n,h}\,,\, u^{h,n}\big)_{\Omega_H} + \big(I_{\text{app}}^{i,n,h} - I_{\text{app}}^{e,n,h}\,,\, u_e^{h,n}\big)_{\Omega_H} \\
&\quad + \big(\mathcal{I}^h, u_e^h\big)_{\omega} \\
&\le \frac{\beta c_m}{4\Delta t} \left\|u^{h,n}\right\|_{L^2(\Omega_H)}^2 + \frac{C_M}{2} \left\|\nabla u_e^{h,n}\right\|_{L^2(\Omega_H)}^2 + C,
\end{aligned} \tag{3.5}
$$

for some constant $C > 0$. Moreover, from (2.3) and Young inequality, we obtain

$$
\big(\beta \tilde{I}_{1,\text{ion}}(u^{h,n})\,,\, u^{h,n}\big)_{\Omega_H} - \beta \big(L\, u^{h,n} + l\,,\, u^{h,n}\big)_{\Omega_H} \ge -\beta \left(\frac{c_m}{4\Delta t} + L \right) \left\|u^{h,n}\right\|_{L^2(\Omega_H)}^2 + C', \tag{3.6}
$$

for some constant C'. Additionally, we deduce from (2.2)

$$\left(\beta I_{2,\mathrm{ion}}(w^{h,n})\,,\,u^{h,n}\right)_{\Omega_H} - (\alpha_4 H(u^{h,n},w^{h,n}),w^{h,n})_{\Omega_H} \geq \alpha_5 \left\|w^{h,n}\right\|^2_{L^2(\Omega_H)}. \tag{3.7}$$

In view of (3.5), (3.6), (3.7), and (2.1), it follows that from (3.4)

$$\begin{aligned}
[\mathcal{A}(\mathbf{u}_h^n),\mathbf{u}_h^n] \geq & \beta\left(\frac{c_m}{2\Delta t} - L\right)\left\|u^{h,n}\right\|^2_{L^2(\Omega_H)} + \frac{\alpha_4}{2\Delta t}\left\|w^{h,n}\right\|^2_{L^2(\Omega_H)} \\
& + C_M\left\|\nabla u_i^{h,n}\right\|^2_{L^2(\Omega_H)} + \frac{C_M}{2}\left\|\nabla u_e^{h,n}\right\|^2_{L^2(\Omega_H)} + C_M\left\|\nabla u_s^{h,n}\right\|^2_{L^2(\Omega_B)} \\
& + \alpha_5\left\|w^{h,n}\right\|^2_{L^2(\Omega_H)} - C(\beta,c_m,\Delta t)\left\|u^{h,n-1}\right\|^2_{L^2(\Omega_H)} - C(\alpha_4,\Delta t)\left\|w^{h,n-1}\right\|^2_{L^2(\Omega_H)} \\
& - C + C'.
\end{aligned}$$

This implies that

$$\begin{aligned}
[\mathcal{A}(\mathbf{u}_h^n),\mathbf{u}_h^n] \geq & \min\left\{\beta\left(\frac{c_m}{2\Delta t} - L\right), \frac{\alpha_4}{2\Delta t}, \frac{C_M}{2}, \alpha_5\right\}\left\|\mathbf{u}_h^{n+1}\right\|^2_{E_h} \\
& - C(\beta,c_m,\Delta t)\left\|u^{h,n-1}\right\|^2_{L^2(\Omega_H)} - C(\alpha_4,\Delta t)\left\|w^{h,n-1}\right\|^2_{L^2(\Omega_H)} - C + C'.
\end{aligned} \tag{3.8}$$

Finally, using the condition $\dfrac{c_m}{2\Delta t} > L$, then for a given , $\mathbf{u}_h^n$ we deduce from (3.8) that (3.3) hold for r large enough (recall that $\left\|\mathbf{u}_h^{n+1}\right\|_{E_h} = r$). Hence, we obtain the existence of at least one solution to the finite element scheme (3.2).

3.3. A priori estimates. In this section we establish several a priori (discrete energy) estimates for the finite element scheme, which eventually will imply the desired convergence results.

PROPOSITION 3.2. *Let $\mathbf{u}_h^n = \left(u_i^{h,n}, u_e^{h,n}, u^{h,n}, u_s^{h,n}, w^{h,n}\right)$ be a solution of the finite element scheme* (3.2)*. Then there exist a constant $C > 0$, depending on Ω_H, Ω_B, T, u_0, w_0, $\mathcal{I}$ and I^j_{app} (for $j = i, e$) such that*

$$\begin{aligned}
\|u^h\|_{L^\infty(0,T;L^2(\Omega_H))} + \|w^h\|_{L^\infty(0,T;L^2(\Omega_H))} &\leq C, \\
\sum_{j=i,e}\left\|\nabla u_j^h\right\|_{L^2(\Omega_{T,H})} + \left\|\nabla u_s^h\right\|_{L^2(\Omega_{T,B})} &\leq C, \\
\sum_{j=i,e}\|u_j^h\|_{L^2(\Omega_{T,H})} + \|u_s^h\|_{L^2(\Omega_{T,B})} + \|u^h\|_{L^r(\Omega_{T,H})} &\leq C.
\end{aligned} \tag{3.9}$$

Proof. We use (3.2) with $\phi_i^h = u_i^{h,n}$, $\phi_e^h = -u_e^{h,n}$, $\phi_s^h = u_s^{h,n}$ and $\varphi^h = w^{h,n}$, and we sum over $n = 1,\ldots,k$ for all $1 < k \leq N$. The result is

$$\begin{aligned}
& \frac{1}{2}\beta c_m(u^{h,k},u^{h,k})_{\Omega_H} + \frac{1}{2}(w^{h,k},w^{h,k})_{\Omega_H} + \beta\int_0^{k\Delta t}\int_{\Omega_H}\tilde{I}_{1,\mathrm{ion}}(u^h)\,u^h \\
& \qquad + C_M\int_0^{k\Delta t}\int_{\Omega_H}\left(\left|\nabla u_i^h\right|^2 + \left|\nabla u_e^h\right|^2\right) + C_M\int_0^{k\Delta t}\int_{\Omega_B}\left|\nabla u_s^h\right|^2 \\
& \leq \frac{1}{2}\beta c_m(u^{h,0},u^{h,0})_{\Omega_H} + \frac{1}{2}(w^{h,0},w^{h,0})_{\Omega_H} + \int_0^{k\Delta t}\int_{\Omega_H}\left(I^{i,h}_{\mathrm{app}}\,u_i^h - I^{e,h}_{\mathrm{app}}\,u_e^h\right) \\
& \quad + \int_0^{k\Delta t}\int_\omega \mathcal{I}^h u_e^h - \beta\int_0^{k\Delta t}\int_{\Omega_H} I_{2,\mathrm{ion}}(w^h)\,u^h + \int_0^{k\Delta t}\int_{\Omega_H} H(u^h,w^h)\,w^h + \int_0^{k\Delta t}\int_{\Omega_H}(L\,u^h + l)\,u^h.
\end{aligned}$$

Herein, we have used the positivity of $\mathbf{M}_{i,e}^h$ and the convexity inequality $a(a-b) \geq \frac{1}{2}(a^2-b^2)$. Using the trace embedding theorem, the Poincare inequality and the Cauchy-Schwarz inequality, yields

(3.10)
$$\begin{aligned}\int_0^{k\Delta t}\int_{\Omega_H}(I_{\rm app}^{i,h}\,u_i^h - I_{\rm app}^{e,h}\,u_e^h)+\int_0^{k\Delta t}\int_\omega \mathcal{I}^h u_e^h &= \int_0^{k\Delta t}\int_{\Omega_H} I_{\rm app}^{i,h}\,u^h + \int_0^{k\Delta t}\int_{\Omega_H}(I_{\rm app}^{i,h}-I_{\rm app}^{e,h})\,u_e^h \\ &\quad + \int_0^{k\Delta t}\int_\omega \mathcal{I}^h u_e^h \\ &\leq C_1\left\|u^h\right\|^2_{L^2(\Omega_{T,H})} + \frac{C_M}{2}\left\|\nabla u_e^h\right\|^2_{L^2(\Omega_{T,H})} + C_2,\end{aligned}$$

for some constants $C_1, C_2 > 0$. Collecting the previous inequalities and using Young inequality, we obtain

$$\begin{aligned}&\frac{1}{2}\beta c_m\left\|u^{h,k}\right\|_{L^2(\Omega_H)} + \frac{1}{2}\left\|w^{h,k}\right\|_{L^2(\Omega_H)} + \beta\int_0^{k\Delta t}\int_{\Omega_H}\tilde{I}_{1,\rm ion}(u^h)\,u^h \\ &\quad + C_M\int_0^{k\Delta t}\int_{\Omega_H}\left|\nabla u_i^h\right|^2 + \frac{C_M}{2}\int_0^{k\Delta t}\int_{\Omega_H}\left|\nabla u_e^h\right|^2 + C_M\int_0^{k\Delta t}\int_{\Omega_B}\left|\nabla u_s^h\right|^2 \\ &\leq \frac{1}{2}\beta c_m\left\|u_0\right\|_{L^2(\Omega_H)} + \frac{1}{2}\left\|w_0\right\|_{L^2(\Omega_H)} + C_3\left\|u^h\right\|^2_{L^2(\Omega_{T,H})} + C_4\left\|w^h\right\|^2_{L^2(\Omega_{T,H})} + C_5,\end{aligned} \tag{3.11}$$

for some constants $C_3, C_4, C_5 > 0$. This implies

$$\frac{1}{2}\beta c_m\left\|u^{h,k}\right\|_{L^2(\Omega_H)} + \frac{1}{2}\left\|w^{h,k}\right\|_{L^2(\Omega_H)} \leq C_3\left\|u^h\right\|^2_{L^2(\Omega_{T,H})} + C_4\left\|w^h\right\|^2_{L^2(\Omega_{T,H})} + C_6, \tag{3.12}$$

for some constant $C_6 > 0$. Therefore by the discrete Gronwall inequality, yields from (3.12) : there exist a constant $C_7 > 0$ such that:

$$\|u^h\|_{L^\infty(0,T;L^2(\Omega_H))} + \|w^h\|_{L^\infty(0,T;L^2(\Omega_H))} \leq C_8, \tag{3.13}$$

for some constant $C_8 > 0$. Using (3.13) in (3.11) and (2.2), we get

$$\|u^h\|_{L^r(\Omega_{T,H})} + \sum_{j=i,e}\left\|\nabla u_j^h\right\|_{L^2(\Omega_{T,H})} + \left\|\nabla u_s^h\right\|_{L^2(\Omega_{T,B})} \leq C_9, \tag{3.14}$$

for some constant $C_9 > 0$. Finally, we obtain from the Poincare inequality

$$\sum_{j=i,e}\|u_j^h\|_{L^2(\Omega_{T,H})} + \|u_s^h\|_{L^2(\Omega_{T,B})} \leq C_{10}, \tag{3.15}$$

for some constant $C_{10} > 0$. This concludes the proof of Lemma 3.2. □

3.4. L^2-Space and time translation estimates. In this section we derive estimates on differences of space and time translates of the functions u^h and w^h which imply that the sequences u^h and w^h are relatively compact in $L^2(\Omega_{T,H})$.

LEMMA 3.2. *There exists a positive constant $C > 0$ depending on Ω_H, T, u_0 and $I_{\rm app}^j$ such that*

$$\begin{aligned}&\iint_{\Omega_H'\times(0,T)}\left[\left|u^h(t,x+\boldsymbol{r})-u^h(t,x)\right|^2 + \left|w^h(t,x+\boldsymbol{r})-w^h(t,x)\right|^2\right]dx\,dt \\ &\qquad\qquad \leq \mathcal{C}\,|\boldsymbol{r}|^2 + T\sup_{0<|\boldsymbol{r}|\leq\delta}\int_{\Omega_{\boldsymbol{r}}}|J^{\boldsymbol{r}}w_0^h|^2,\end{aligned} \tag{3.16}$$

for all $\boldsymbol{r} \in \mathbb{R}^3$ with $\Omega_H' = \{x \in \Omega_H,\, [x, x+r] \subset \Omega_H\}$, and

$$\iint_{\Omega_H\times(0,T-\tau)}\left[\left|u^h(t+\tau,x)-u^h(t,x)\right|^2 + \left|w^h(t+\tau,x)-w^h(t,x)\right|^2\right]dx\,dt \leq C(\tau+\Delta t). \tag{3.17}$$

for all $\tau \in (0,T)$.

Proof. In the first step we provide the *proof of estimate* (3.16). In this regard, we start with the uniform estimate of space translate of u^h from the uniform L^2 estimate of ∇u^h. We let the space translate $(J^{\boldsymbol{r}}u^h)(\cdot,\boldsymbol{x}) = u^h(\cdot,\boldsymbol{x}+\boldsymbol{r}) - u^h(\cdot,\boldsymbol{x})$. Observe that from $L^2(0,T;H^1(\Omega_H))$, we get easily the estimate of u^h (recall that $\boldsymbol{r} \in \mathbb{R}^3$ and $\Omega_{\boldsymbol{r}} := \{\boldsymbol{x} \in \Omega \,|\, \boldsymbol{x}+\boldsymbol{r} \in \Omega\}$):

$$\int_0^T \int_{\Omega_{\boldsymbol{r}}} |J^{\boldsymbol{r}}u^h|^2 \leq \mathcal{C}|\boldsymbol{r}|^2. \tag{3.18}$$

It is clear that the right-hand side in (3.18) vanishes as $|\boldsymbol{r}| \to 0$, uniformly in h. Along the same lines as u^h, we get the space translation for w^h.

Now we furnish the *Proof of* (3.17). We introduce the time translates functions

$$(T^h u^h)(t,\cdot) := u^h(t+\tau,\cdot) - u^h(t,\cdot) \text{ and } (T^h w^h)(t,\cdot) := w^h(t+\tau,\cdot) - w^h(t,\cdot).$$

Observe that for all $t \in [0, T-\tau]$ these functions take values in V_H^h. Therefore they can be used as test functions in the weak formulations (3.2). Moreover we previously proved uniform in h bounds on w^h and ∇u^h in $L^2(\Omega_{T,H})$ and on u^h in $L^r(\Omega_{T,H})$. This implies the analogous bounds for the translates $T^\tau w^h$ and $\nabla T^\tau u^h$ in $L^2((0,T-\tau)\times\Omega_H)$ and $T^\tau u^h$ in $L^r((0,T-\tau)\times\Omega_H)$.

To prove the time translation estimates, we introduce $\bar{u}^h$ and $\bar{w}^h$ the piecewise affine in t functions in $W^{1,\infty}([0,T];V_H^h)$ interpolating the states $(u^{h,n})_{=n=0..N} \subset V_H^h$ and $(w^h)_{n=0..N} \subset V_H^h$ at the points $(n\Delta t)_{n=0..N}$. Then we have

$$\begin{cases} \beta c_m \partial_t \bar{u}^h - \nabla\cdot\,(\mathbf{M}_{\rm i}(x)\nabla u_i^h) + \beta I_{\rm ion}(u^h,w^h) = I_{\rm app}^i & (t,x) \in \Omega_{T,H}, \\ \beta c_m \partial_t \bar{u}^h + \nabla\cdot\,(\mathbf{M}_{\rm e}(x)\nabla u_e^h) + \beta I_{\rm ion}(u^h,w^h) = I_{\rm app}^e & (t,x) \in \Omega_{T,H}, \\ -\nabla\cdot\,(\mathbf{M}_{\rm s}(x)\nabla u_s^h) = 0 & (t,x) \in \Omega_{T,B}, \\ \partial_t \bar{w}^h - H(u^h,w^h) = 0 & (t,x) \in \Omega_{T,H}. \end{cases} \tag{3.19}$$

We integrate the approximations of (3.19) with respect to the time parameter $s \in [t, t+\tau]$ (with $0 < \tau < T$). In the resulting equations, we take the test functions as the corresponding translates $T^\tau u_i^h$, $-T^\tau u_e^h$, $T^\tau u_s^h$

and $T^\tau w^h$, respectively. The result is

$$
\begin{aligned}
&\int_0^{T-\tau}\int_{\Omega_H}\left|(T^h\bar u^h)(t,x)\right|^2\,dx\,dt+\int_0^{T-\tau}\int_{\Omega_H}\left|(T^h\bar w^h)(t,x)\right|^2\,dx\,dt\\
&\quad=\int_0^{T-\tau}\int_{\Omega_H}\left(\int_t^{t+\tau}\partial_s\bar u^h(s,x)\,ds\right)(T^hu^h)(t,x)\,dx\,dt\\
&\qquad+\int_0^{T-\tau}\int_{\Omega_H}\left(\int_t^{t+\tau}\partial_s\bar w^h(s,x)\,ds\right)(T^hw^h)(t,x)\,dx\,dt\\
&\quad=-\sum_{j=i,e}\int_0^{T-\tau}\int_{\Omega_H}\int_t^{t+\tau}\mathbf{M}_{\rm j}(x)\nabla u_j^h(s,x)\cdot\nabla(T^hu_j^h)(t,x)\,dx\,ds\,dt\\
&\qquad-\int_0^{T-\tau}\int_{\Omega_B}\int_t^{t+\tau}\mathbf{M}_{\rm s}(x)\nabla u_s^h(s,x)\cdot\nabla(T^hu_s^h)(t,x)\,dx\,ds\,dt\\
&\qquad-\int_0^{T-\tau}\int_{\omega}\int_t^{t+\tau}\mathcal{I}^h(T^hu_e^h)(t,x)\,dx\,ds\,dt\\
&\qquad-\int_0^{T-\tau}\int_{\Omega_H}\int_t^{t+\tau}I_{\rm ion}(u^h(s,x),w^h(s,x))(T^hu^h)(t,x)\,dx\,ds\,dt\\
&\qquad+\int_0^{T-\tau}\int_{\Omega_H}\int_t^{t+\tau}H(u^h(s,x),w^h(s,x))(T^hw^h)(t,x)\,dx\,ds\,dt\\
&\qquad+\sum_{j=i,e}\int_0^{T-\tau}\int_{\Omega_H}\int_t^{t+\tau}\left(I^{i,h}_{\rm app}(T^hu_i^h)(t,x)-I^{e,h}_{\rm app}(T^hu_e^h)(t,x)\right)dx\,ds\,dt\\
&\quad=I_1+I_2+I_3+I_4+I_5+I_6.
\end{aligned}
\tag{3.20}
$$

Now we examine these integrals separately. For the term I_1, we have

$$
\begin{aligned}
|I_1|&\le C\sum_{j=i,e}\left[\int_0^{T-\tau}\int_{\Omega_H}\left(\int_t^{t+\tau}\left|\nabla u_j^h(s,x)\right|^2\,ds\right)^2dx\,dt\right]^{\frac12}\times\left[\int_0^{T-\tau}\int_{\Omega_H}\left|\nabla(T^hu_j^h)(t,x)\right|^2\,dx\,dt\right]^{\frac12}\\
&\le C\,\tau,
\end{aligned}
\tag{3.21}
$$

and similarly

$$
|I_2|+|I_3|\le C\,\tau
$$

for some constant $C>0$. Herein we used the Fubini theorem (recall that $\int_t^{t+\tau}ds=\tau=\int_{s-\tau}^{s}dt$), the Hölder inequality and the bounds in L^2 of $\mathcal{I}^h$, u_j^h, ∇u_j^h and $\nabla T^hu_j^h$ for $j=i,e,s$. Keeping in mind the growth bound of the nonlinearity $I_{\rm ion}$, we apply the Hölder inequality (with $p=r$, $p'=r/(r-1)$ in the ionic current term and with $p=p'=2$ in the other ones) to deduce (note that (u^h,T^hu^h) and w^h are uniformly bounded in L^r and L^2, respectively)

$$
\begin{aligned}
|I_4|&\le C\Bigg(\left[\int_0^{T-\tau}\int_{\Omega_H}\left(\int_t^{t+\tau}\left|u^h(s,x)\right|^r\,ds\right)^2dx\,dt\right]^{\frac{r-1}{r}}\times\left[\int_0^{T-\tau}\int_{\Omega_H}\left|(T^hu^h)(t,x)\right|^r\,dx\,dt\right]^{\frac1r}\\
&\qquad+\left[\int_0^{T-\tau}\int_{\Omega_H}\left(\int_t^{t+\tau}\left|w^h(s,x)\right|^2\,ds\right)^2dx\,dt\right]^{\frac12}\times\left[\int_0^{T-\tau}\int_{\Omega_H}\left|(T^hu^h)(t,x)\right|^2\,dx\,dt\right]^{\frac12}\Bigg)\\
&\le C\,\tau,
\end{aligned}
\tag{3.22}
$$

for some constant $C>0$. Analogously we obtain

$$
|I_5|+|I_6|\le C\,\tau,
$$

for some constant $C > 0$. Collecting the previous inequalities we readily deduce

$$\int_0^{T-\tau}\int_{\Omega_H}\left(|\bar{u}^h(t+\tau,\cdot)-\bar{u}^h(t,\cdot)|^2+|\bar{w}^h(t+\tau,\cdot)-\bar{w}^h(t,\cdot)|^2\right)\leq \mathcal{C}\,\tau.$$

Further, it is easily seen from the definition of $(\bar{u}^h,\bar{w}^h)$ and from the system

$$\begin{cases}\beta c_m\dfrac{u^{h,n}-u^{h,n-1}}{\Delta t}-\nabla\cdot\left(\mathbf{M}_{\rm i}(x)\nabla u_i^h\right)+\beta I_{\rm ion}(u^h,w^h)=I_i & (t,x)\in\Omega_{T,H},\\ \beta c_m\dfrac{u^{h,n}-u^{h,n-1}}{\Delta t}+\nabla\cdot\left(\mathbf{M}_{\rm e}(x)\nabla u_e^h\right)+\beta I_{\rm ion}(u^h,w^h)=I_e & (t,x)\in\Omega_{T,H},\\ \dfrac{w^{h,n}-w^{h,n-1}}{\Delta t}-H(u^h,w^h)=0 & (t,x)\in\Omega_{T,H}.\end{cases}\tag{3.23}$$

and estimates in Proposition 3.2 that

$$\|\bar{u}^h-u^h\|^2_{L^2(\Omega_{T,H})}\leq\sum_{n=1}^N\Delta t\|u^{h,n}-u^{h,n-1}\|^2_{L^2(\Omega_H)}\leq\mathcal{C}(\Delta t)\to 0\ \text{ as }\Delta t\to 0,$$

and

$$\|\bar{w}^h-w^h\|^2_{L^2(\Omega_{T,H})}\leq\sum_{n=1}^N\Delta t\|w^{h,n}-w^{h,n-1}\|^2_{L^2(\Omega_H)}\leq\mathcal{C}(\Delta t)\to 0\ \text{ as }\Delta t\to 0.$$

This concludes the proof of Lemma 3.2.
□

3.5. Convergence of the finite element scheme. The next lemma is a consequence of Lemma 3.2 and Kolmogorov's compactness criterion (see, e.g., [9], Theorem IV.25).

LEMMA 3.3. *There exists a subsequence of* $\mathbf{u}_h=(u_{i,h},u_{e,h},u_h,u_{s,h},w_h)$*, not relabeled, such that, as* $h\to 0$*,*

$$\begin{aligned}&u_h\to u \text{ strongly in } L^2(\Omega_{T,H}) \text{ and a.e. in } \Omega_{T,H},\\ &w_h\to w \text{ strongly in } L^2(\Omega_{T,H}) \text{ and a.e. in } \Omega_{T,H},\\ &u_h\rightharpoonup u \text{ weakly in } L^2(0,T;H^1(\Omega_H)),\\ &u_{i,h}\rightharpoonup u_i \text{ weakly in } L^2(0,T;\tilde{H}^1(\Omega_H)),\\ &u_{e,h}\rightharpoonup u_e \text{ weakly in } L^2(0,T;\tilde{H}^1(\Omega_H)),\\ &u_{s,h}\rightharpoonup u_s \text{ weakly in } L^2(0,T;H^1(\Omega_B)),\\ &u_h\rightharpoonup u \text{ weakly in } L^r(\Omega_{T,H}),\end{aligned}\tag{3.24}$$

where $u=u_i-u_e$. With the above convergences, we are ready to identify the limit $\mathbf{u}=(u_i,u_e,u,u_s,w)$ as a (weak) solution of the system (1.1). Finally, let $\varphi_i,\varphi_e\in L^2(0,T,H^1(\Omega_H))\cap L^r(\Omega_{T,H})$, $\varphi_s\in L^2(0,T,H^1(\Omega_B))$ and $\varphi_w\in C([0,T],L^2(\Omega_H))$ with $\varphi_e=\varphi_s$ on Σ_H, then by passing to the limit $h\to 0$ in the following weak formulation (with the help of Lemma 3.3)

$$\begin{aligned}\iint_{\Omega_{T,H}}\beta c_m\partial_t\bar{u}^h(t,x)\varphi_i+\iint_{\Omega_{T,H}}\mathbf{M}_{\rm i}(x)\nabla u_i^h(x,t)\nabla\varphi_i+\iint_{\Omega_{T,H}}\beta I^\epsilon_{\rm ion}(u^h,w^h)\varphi_i&=\iint_{\Omega_{T,H}}I^{i,h}_{\rm app}\phi_i\\ \iint_{\Omega_{T,H}}\beta c_m\partial_t\bar{u}^h(t,x)\varphi_e-\iint_{\Omega_{T,H}}\mathbf{M}_{\rm e}(x)\nabla u_e^h(x,t)\nabla\varphi_e+\iint_{\Omega_{T,B}}\mathbf{M}_{\rm s}(x)\nabla u_s^h(x,t)\nabla\varphi_s&\\ -\iint_{\Sigma_{1,T}}\mathcal{I}^h\varphi_e+\iint_{\Omega_{T,H}}\beta I^\epsilon_{\rm ion}(u^h,w^h)\varphi_e&=\iint_{\Omega_{T,H}}I^{e,h}_{\rm app}\varphi_e\end{aligned}$$

$$\iint_{\Omega_{T,H}} \partial_t \bar{w}^h(t,x)\varphi_w - H(u^h, w^h)\varphi_w = 0,$$

in this way we obtain the limit $\mathbf{u} = (u_i, u_e, u, u_s, w)$ which is a solution of system (1.1) in the sense of Definition 2.1.

3.6. Uniqueness of the weak solution. The purpose is to prove uniqueness of the weak solution to our degenerate problem (1.1). In our uniqueness proof, we will need the following technical lemma (where the proof is given in [2]) adapted to the weak formulation of Definition 2.1.

LEMMA 3.4. *There exists a family of linear operators $(\Theta_\epsilon)_{\epsilon>0}$ from $L^2(0,T,H^1(\Omega_H))$ into $\mathcal{C}_c^\infty(\mathbb{R}\times\mathbb{R}^d)$ such that - for all $u \in L^2(0,T,H^1(\Omega_H))$, $\Theta_\epsilon(u)$ converges to u in $L^2(0,T,H^1(\Omega_H))$;*
- for all $u \in L^r(\Omega_{T,H}) \cap L^2(0,T,H^1(\Omega_H))$, $\Theta_\epsilon(u)$ converges to u in $L^r(\Omega_{T,H})$.

REMARK 3.1. *Note that Lemma 3.4 is used to regularize u_i and u_e (recall that $u_i, u_e \in L^2(0,T,H^1(\Omega_H))$ and $u_i, u_e \notin L^r(\Omega_{T,H})$), so that one can take $\Theta_\epsilon(u_i)$ and $\Theta_\epsilon(u_e)$ as test functions in* (2.5). An application of Lemma 3.4 is the following uniqueness result:

THEOREM 3.5. *Assume that the initial and bounded conditions (1.1) and (2.1)- (2.3) are satisfied. Let $(u_{i,1}, u_{e,1}, u_{s,1}, u_1, w_1)$ and $(u_{i,2}, u_{e,2}, u_{s,2}, u_2, w_2)$ be two weak solutions to the (1.1) model. Then for any $t \in [0,T]$, there exists a constant $C > 0$ such that*

$$\begin{aligned}
&\int_{\Omega_H} |(u_1-u_2)(t)|^2 + \int_{\Omega_H} |(w_1-w_2)(t)|^2 + \int_0^t \int_{\Omega_B} |u_{s,1}-u_{s,2}|^2 \\
&\qquad \le C\Big(\int_0^t \int_\omega |\mathcal{I}_1 - \mathcal{I}_2|^2 + \int_0^t \int_{\Omega_H} \left|I_{\text{app}}^{i,2} - I_{\text{app}}^{i,1}\right|^2 + \int_0^t \int_{\Omega_H} \left|I_{\text{app}}^{e,2} - I_{\text{app}}^{e,1}\right|^2 + \int_{\Omega_H} |u_{1,0}-u_{2,0}|^2 \\
&\qquad\qquad + \int_{\Omega_H} |w_{1,0}-w_{2,0}|^2 \Big).
\end{aligned}$$

In particular, there exists at most one weak solution to the model (1.1). **Proof** Note that the following equations hold for all test functions $\phi_j \in L^2(0,T;H^1(\Omega_H)), j = i,e$, $\phi_s \in L^2(0,T;H^1(\Omega_B))$, and $\phi_w \in C(0,T;L^2(\Omega_H))$:

$$\begin{aligned}
&\int_{\Omega_H} \beta c_m \partial_t(u_1-u_2)\phi_i + \int_{\Omega_H} \mathbf{M}_\text{i}\nabla(u_{i,1}-u_{i,2})\cdot\nabla\phi_i + \int_{\Omega_H} \beta(I_{\text{ion}}(u_1,w_1) - I_{\text{ion}}(u_2,w_2))\phi_i \\
&\qquad\qquad = \int_{\Omega_H} (I_{\text{app}}^{i,1} - I_{\text{app}}^{i,2})\phi_i, \\
&\int_{\Omega_H} \beta c_m \partial_t(u_1-u_2)\phi_e - \int_{\Omega_H} \mathbf{M}_\text{e}\nabla(u_{e,1}-u_{e,2})\cdot\nabla\phi_e + \int_{\Omega_B} \mathbf{M}_\text{s}\nabla(u_{s,1}-u_{s,2})\cdot\nabla\phi_s \\
&\qquad - \int_\omega (\mathcal{I}_1 - \mathcal{I}_2)\phi_s + \int_{\Omega_H} \beta(I_{\text{ion}}(u_1,w_1) - I_{\text{ion}}(u_2,w_2))\phi_e = \int_{\Omega_H} (I_{\text{app}}^{e,1} - I_{\text{app}}^{e,2})\phi_e, \\
&\int_{\Omega_H} \partial_t(w_1-w_2)\phi_w = \int_{\Omega_H} (H(u_1,w_1) - H(u_2,w_2))\phi_w.
\end{aligned}$$

Substituting $\phi_i = \Theta_\epsilon(u_{i,1}-u_{i,2})$, $\phi_e = -\Theta_\epsilon(u_{e,1}-u_{e,2})$,$\phi_s = u_{s,1}-u_{s,2}$, $\phi_w = w_1 - w_2$ in the equations. We subtract the resulting equations and apply the technical Lemma 3.4; using the linearity of

$\Theta_\epsilon(\cdot)$, sending $\epsilon \to 0$ and integrating in time $(0,t)$ for $0 < t \leq T$, we arrive at

$$\begin{aligned}
&\int_{\Omega_H} \frac{\beta c_m}{2} |(u_1-u_2)(t)|^2 + \int_{\Omega_H} \frac{1}{2} |(w_1-w_2)(t)|^2 + \sum_{j=i,e} \int_0^t \int_{\Omega_H} \mathbf{M}_{\mathrm{j}} \nabla(u_{j,1}-u_{j,2}) \cdot \nabla(u_{j,1}-u_{j,2}) \\
&\quad + \int_0^t \int_{\Omega_B} \mathbf{M}_{\mathrm{s}} \nabla(u_{s,1}-u_{s,2}) \cdot \nabla(u_{s,1}-u_{s,2}) + \int_0^t \int_{\Omega_H} \beta(I_{\mathrm{ion}}(u_1,w_1) - I_{\mathrm{ion}}(u_2,w_2))(u_1-u_2) \\
&= \int_0^t \int_\omega (\mathcal{I}_1 - \mathcal{I}_2)(u_{e,1}-u_{e,2}) + \int_0^t \int_{\Omega_H} (H(u_1,w_1) - H(u_2,w_2))(w_1-w_2) \\
&\quad + \int_{\Omega_H} \frac{\beta c_m}{2} |u_{1,0}-u_{2,0}|^2 + \int_{\Omega_H} \frac{1}{2} |w_{1,0}-w_{2,0}|^2 + \int_0^t \int_{\Omega_H} (I^{i,1}_{\mathrm{app}} - I^{i,2}_{\mathrm{app}})(u_{i,1}-u_{i,2}) \\
&\quad - \int_0^t \int_{\Omega_H} (I^{e,1}_{\mathrm{app}} - I^{e,2}_{\mathrm{app}})(u_{e,1}-u_{e,2}).
\end{aligned}$$

Now we use (2.1), (2.2), (2.3), (2.4), (1.6), Young inequality and the trace embedding theorem to deduce

$$\begin{aligned}
&\int_{\Omega_H} \frac{\beta c_m}{2} |(u_1-u_2)(t)|^2 + \int_{\Omega_H} \frac{1}{2} |(w_1-w_2)(t)|^2 + C_M \int_0^t \int_{\Omega_B} |\nabla u_{i,1} - \nabla u_{i,2}|^2 \\
&\qquad + \frac{C_M}{2} \int_0^t \int_{\Omega_B} |\nabla u_{e,1} - \nabla u_{e,2}|^2 + C_M \int_0^t \int_{\Omega_B} |\nabla u_{s,1} - \nabla u_{s,2}|^2 \\
&\leq C\Big(\int_0^t \int_{\Omega_H} |u_1-u_2|^2 + \int_0^t \int_{\Omega_H} |w_1-w_2|^2 + \int_0^t \int_\omega |\mathcal{I}_1-\mathcal{I}_2|^2 + \int_0^t \int_{\Omega_H} \left|I^{i,2}_{\mathrm{app}} - I^{i,1}_{\mathrm{app}}\right|^2 \\
&\qquad + \int_0^t \int_{\Omega_H} \left|I^{e,2}_{\mathrm{app}} - I^{e,1}_{\mathrm{app}}\right|^2 + \int_{\Omega_H} |u_{1,0}-u_{2,0}|^2 + \int_{\Omega_H} |w_{1,0}-w_{2,0}|^2 \Big),
\end{aligned}$$

for some constant $C > 0$. Using this and Poincaré inequality, we obtain

$$\begin{aligned}
&\int_{\Omega_H} \frac{\beta c_m}{2} |(u_1-u_2)(t)|^2 + \int_{\Omega_H} \frac{1}{2} |(w_1-w_2)(t)|^2 + C_p \int_0^t \int_{\Omega_B} |u_{s,1} - u_{s,2}|^2 \\
&\leq C\Big(\int_0^t \int_{\Omega_H} |u_1-u_2|^2 + \int_0^t \int_{\Omega_H} |w_1-w_2|^2 + \int_0^t \int_\omega |\mathcal{I}_1-\mathcal{I}_2|^2 + \int_0^t \int_{\Omega_H} \left|I^{i,2}_{\mathrm{app}} - I^{i,1}_{\mathrm{app}}\right|^2 \\
&\qquad + \int_0^t \int_{\Omega_H} \left|I^{e,2}_{\mathrm{app}} - I^{e,1}_{\mathrm{app}}\right|^2 + \int_{\Omega_H} |u_{1,0}-u_{2,0}|^2 + \int_{\Omega_H} |w_{1,0}-w_{2,0}|^2 \Big),
\end{aligned}$$

for some constant $c_p > 0$. Finally an application of Gronwall inequality yields

$$\begin{aligned}
&\int_{\Omega_H} |(u_1-u_2)(t)|^2 + \int_{\Omega_H} |(w_1-w_2)(t)|^2 + \int_0^t \int_{\Omega_B} |u_{s,1} - u_{s,2}|^2 \\
&\qquad \leq C\Big(\int_0^t \int_\omega |\mathcal{I}_1-\mathcal{I}_2|^2 + \int_0^t \int_{\Omega_H} \left|I^{i,2}_{\mathrm{app}} - I^{i,1}_{\mathrm{app}}\right|^2 + \int_0^t \int_{\Omega_H} \left|I^{e,2}_{\mathrm{app}} - I^{e,1}_{\mathrm{app}}\right|^2 + \int_{\Omega_H} |u_{1,0}-u_{2,0}|^2 \\
&\qquad\qquad + \int_{\Omega_H} |w_{1,0}-w_{2,0}|^2 \Big).
\end{aligned}$$

for some constant $C > 0$. This completes the uniqueness theorem.

4. Optimal control of the heart activity. In this section, the optimal control framework for the cardiac defibrillation is described. The existence of the control, the complete optimality system and the existence of the Lagrange multipliers are shown.

4.1. Existence of the control. In this subsection, we provide the existence of the solution for the optimal control problem of the bidomain-bath model equations. We considered the following cost functional for the optimization of the cardiac defibrillation.

$$(4.1\mathcal{P}) \quad \begin{cases} \min_{\mathcal{I}} \left[J(u,\mathcal{I}) = \frac{1}{2}\left(\epsilon_1 \iint_{\Omega_{T,H}} |u(x,t) - u_d(x,t)|^2 \, dx\, dt + \epsilon_2 \iint_{\Sigma_{1,T}} \mathcal{I}(s,t)^2 \, ds\, dt \right) \right], \\ \text{subject to the coupled bidomain-bath system (1.1).} \end{cases}$$

Here ϵ_1 and ϵ_2 are the regularization parameters and u_d is the desired state solution at the cardiac tissue domain. The main idea is to compute the optimal control such a way that the arrhythmia pattern moves as close as to the desired state solution. In this work, the placement of the electrodes is located at the boundary of the cardiac tissue domain which is also shared by the part of bath boundary, as shown in Figure 1. Here $\omega := \Gamma_1 \cup \Gamma_2$ is the stimulation boundary. Introducing the following reduced cost functional as follows

$$\hat{J}(\mathcal{I}) := J(u(\mathcal{I}), \mathcal{I}). \tag{4.2}$$

This reduced cost functional will be used in the following lemma concerning the existence of an optimal solution for (4.2).

LEMMA 4.1. *Given $u_0, w_0 \in L^2(\Omega_H)$, $I^i_{\text{app}}, I^e_{\text{app}} \in L^2(\Omega_{T,H})$ and $u_d \in L^2(\Omega_{T,H})$, there exists a solution $\mathcal{I}^*$ of the optimal control problem (4.2).*

Proof. For the sequence $(\mathbf{u}_n)_n = (u_{i,n}, u_{e,n}, u_n, u_{s,n}, w_n, \mathcal{I}_n)_n$, let $(\mathcal{I}_n)_n$ be a minimizing sequence. Since J is bounded, we deduce from the definition of J that

$$\int_0^T \int_{\omega \subset \Sigma_H} |\mathcal{I}_n(s,t)|^2 \, ds dt \leq C,$$

for some constant $C > 0$. Using this, Theorem 3.1 and Lemma 3.3 to deduce the following convergence (up a subsequence)

$$\begin{aligned} &u_n \to u^* \text{ strongly in } L^2(\Omega_{T,H}) \text{ and a.e. in } \Omega_{T,H}, \\ &w_n \to w^* \text{ strongly in } L^2(\Omega_{T,H}) \text{ and a.e. in } \Omega_{T,H}, \\ &u_n \to u^* \text{ weakly in } L^r(\Omega_{T,H}), \\ &\nabla_h u_{j,n} \to \nabla u_j^* \text{ weakly in } (L^2(\Omega_{T,H}))^3 \text{ for } j = i, e, \\ &\nabla_h u_{s,n} \to \nabla u_s^* \text{ weakly in } (L^2(\Omega_{T,B}))^3, \end{aligned} \tag{4.3}$$

where $u^* = u_i^* - u_e^*$. With this convergence we deduce easily

$$\min_{\mathcal{I}} \hat{J}(\mathcal{I}) \leq \hat{J}(\mathcal{I}^*) \leq \liminf_{n\to\infty} \hat{J}(\mathcal{I}_n) = \min_{\mathcal{I}} \hat{J}(\mathcal{I}).$$

This implies finally that $\mathcal{I}^*$ is an optimal control solution to the problem (4.2). ∎

4.2. Optimal conditions and dual problem. In this subsection, we derive the optimality conditions based on the Lagrangian formulation which is defined as follows:

(4.4)

$$
\begin{aligned}
L(\theta) =& \frac{\epsilon_1}{2}\iint_{\Omega_{T,H}} |u(x,t)-u_d(x,t)|^2\,dx\,dt + \frac{\epsilon_2}{2}\iint_{\Sigma_{1,T}} \mathcal{I}(s,t)^2\,ds\,dt \\
&+ \iint_{\Omega_{H,T}} \big(\beta c_{\mathrm{m}}\partial_t(u_i-u_e) + \beta I_{\mathrm{ion}}(v,w)\big)(p_i-p_e)\,dx\,dt - \iint_{\Omega_{H,T}} \nabla\cdot\,(\mathbf{M}_{\mathrm{i}}(x)\nabla p_i)u_{\mathrm{i}}\,dx\,dt \\
&+ \iint_{\Sigma_{H,T}} (\mathbf{M}_{\mathrm{i}}(y)\nabla p_i)\cdot\eta\,u_{\mathrm{i}}\,dy\,dt + \iint_{\Omega_{H,T}} \nabla\cdot\,(\mathbf{M}_{\mathrm{e}}(x)\nabla p_e)u_{\mathrm{e}}\,dx\,dt \\
&- \iint_{\Sigma_{H,T}} (\mathbf{M}_{\mathrm{e}}(y)\nabla p_e)\cdot\eta\,u_{\mathrm{e}}\,dy\,dt + \int_{\Omega_{B,T}} \nabla\cdot\,(\mathbf{M}_{\mathrm{s}}(x)\nabla p_s)u_{\mathrm{s}}\,dx\,dt \\
&- \iint_{\Sigma_{B,T}} (\mathbf{M}_{\mathrm{s}}(y)\nabla p_s)\cdot\eta_s\,u_{\mathrm{s}}\,dy\,dt - \iint_{\Sigma_{H,T}} (\mathbf{M}_{\mathrm{s}}(y)\nabla p_s)\cdot\eta_s\,u_{\mathrm{s}}\,dy\,dt \\
&+ \iint_{\Omega_{H,T}} \big(\partial_t w - H(u,w)\big)p_w\,dx\,dt + \iint_{\Sigma_{H,T}} \big(u_e-u_s\big)z_1\,dy\,dt \\
&+ \iint_{\Sigma_1} \big(\mathbf{M}_{\mathrm{e}}(y)\nabla u_{\mathrm{e}} - \mathcal{I} - \mathbf{M}_{\mathrm{s}}(y)\nabla u_{\mathrm{s}}\big)\cdot\eta\,z_2\,dy\,dt + \iint_{\Sigma_2} \big(\mathbf{M}_{\mathrm{e}}(y)\nabla u_{\mathrm{e}} - \mathbf{M}_{\mathrm{s}}(y)\nabla u_{\mathrm{s}}\big)\cdot\eta\,z_3\,dy\,dt,
\end{aligned}
$$

where $\theta = (u_i, u_e, u_s, w, I_i, I_e, \mathcal{I}, p_i, p_e, p_s, p_w, z_1, z_2, z_3)$. The first order optimality system characterizing the adjoint variables, is given by the Lagrange multipliers which result from equating the partial derivatives of L with respect to u_i, u_e, u_s and w equal to zero

$$
\text{(4.5)}\quad
\begin{cases}
-\beta c_m\partial_t p - \nabla\cdot\,(\mathbf{M}_i(x)\nabla p_i) + \beta I_{\mathrm{ion}u}(u,w)p - H_u(u,w)p_w + \epsilon_1(u-u_d) = 0 & \text{in } \Omega_{T,H}\ , \\
-\beta c_m\partial_t p + \nabla\cdot\,(\mathbf{M}_e(x)\nabla p_e) + \beta I_{\mathrm{ion}u}(u,w)p + H_u(u,v)p_w - \epsilon_1(u-u_d) = 0 & \text{in } \Omega_{T,H}\ , \\
-\nabla\cdot\,(\mathbf{M}_{\mathrm{s}}(x)\nabla p_s) = 0 & \text{in } \Omega_{T,B}\ , \\
-\partial_t p_w - H_w(u,w)p_w + I_{\mathrm{ion}w}(u,v)p = 0 & \text{in } \Omega_{T,H}\ ,
\end{cases}
$$

completed with the following conditions (boundary and final time) :

$$
\text{(4.6)}\quad
\begin{cases}
p(\cdot,T) = p_T = 0 \text{ and } p_w(\cdot,T) = p_{w,T} = 0 & \text{in } \Omega_H, \\
(\mathbf{M}_i(s)\nabla p_i(s,t))\cdot\eta = 0 & \text{on } \Sigma_{T,H}, \\
(\mathbf{M}_e(s)\nabla p_e(s,t))\cdot\eta = (\mathbf{M}_s(s)\nabla p_s(s,t))\cdot\eta & \text{on } \Sigma_{T,H}, \\
p_e(s,t) = p_s(s,t) & \text{on } \Sigma_{T,H}, \\
(\mathbf{M}_{\mathrm{s}}(s)\nabla p_s(s,t))\cdot\eta_s = 0 & \text{on } \Sigma_{T,B}.
\end{cases}
$$

Herein, $p := p_i - p_e$, $I_{\mathrm{ion}u}$, $I_{\mathrm{ion}w}$, H_u and H_w are the derivatives of I_{ion} and H with respect to u, w, respectively. Note that from (4.6), we have continuity conditions for the adjoint variables and their derivatives on the heart surface. To find the optimal conditions, we calculate the gradient of the functional $J(u,\mathcal{I})$:

$$
(\frac{\partial L}{\partial \mathcal{I}}, \delta I) = \iint_{\Sigma_{1,T}} (\epsilon_2\mathcal{I}(s,t) - p_e(s,t))\delta I ds dt \text{ and } \nabla J(u,\mathcal{I}) = \frac{\partial L}{\partial \mathcal{I}}.
$$

Observe that the optimality condition can be written as follows

$$
\nabla J(u,\mathcal{I}) = 0 \Rightarrow \iint_{\Sigma_{1,T}} (\epsilon_2\mathcal{I}(s,t) - p_e(s,t)) ds dt = 0.
$$

Finally, we introduce the condition of compatibility : we suppose that p_e has a zero-mean:

$$\int_{\Omega_H} p_e(t,x)\,dx = 0 \text{ for all } t \in (0,T). \tag{4.7}$$

We define the solution operator:
$S : L^2(\Sigma_{1,T}) \to L^2(0,T,\tilde{H}^1(\Omega_H))\times L^2(0,T,\tilde{H}^1(\Omega_H))\times L^2(0,T,H^1(\Omega_H))\cap L^r(\Omega_{T,H})\times L^2(0,T,H^1(\Omega_B))\times C([0,T],L^2(\Omega_H))$, by $(u_i,u_e,u,u_s,w) = S(\mathcal{I})$ for $\mathcal{I} \in L^2(\Sigma_{1,T})$ and (u_i,u_e,u,u_s,w) is the solution to (1.1).

PROPOSITION 4.1 (Control to state map). *The control to state mapping $\mathcal{I} \to (u_i,u_e,u,u_s,w)$ is well defined for the problem* (4.5)-(4.6)*.*

Proof. The bidomain-bath model equations in (1.1) together with the assumptions (2.1)-(2.4) and (1.6) and the initial data $u_0 \in L^2(\Omega_H)$, $w_0 \in L^2(\Omega_H)$ and $I^j_{\text{app}} \in L^2(\Omega_{T,H})$ for $j = i,e$, the existence of the weak solution (u_i,u_e,u,u_s,w) is guaranteed for any feasible control $\mathcal{I} \in L^2(\Sigma_{1,T})$ by the Theorem (3.1). □

THEOREM 4.2 (First order necessary optimality conditions). *Let the assumptions* (2.1)-(2.4) *and* (1.6) *hold and $\mathbf{u}^* = (u_s^*,u_e^*,u_i^*,w^*)$ be a local solution to the bidomain-bath model equations* (1.1)*. Then there exists a unique Lagrange multiplier $\mathbf{p}^* = (p_i^*,p_e^*,p^*,p_s^*,p_w^*) \in L^2(0,T,\tilde{H}^1(\Omega_H))\times L^2(0,T,\tilde{H}^1(\Omega_H))\times L^2(0,T,H^1(\Omega_H))\cap L^r(\Omega_{T,H})\times L^2(0,T,H^1(\Omega_B))\times C([0,T],L^2(\Omega_H))$ such that the pair $(p_i^*,p_e^*,p^*p_s^*,p_w^*)$ is a weak solution to the adjoint equations* (4.5)-(4.6)*. Moreover, the optimality condition* (4.7) *holds for almost all $t \in [0,T]$.*

The proof of the above theorem is shown in the following section.

5. Existence of the solution of adjoint problem. In this section, we proof of the existence of the solution of adjoint system. First, we define our weak solution to adjoint problem (4.5)-(4.6):

DEFINITION 5.1 (Weak solution). *A weak solution to the system (1.1) is a five tuple function $(p_i,p_e,p_s,p := p_i - p_e,p_w)$ such that $p \in L^2(0,T,H^1(\Omega_H))$, $p_i,p_e \in L^2(0,T,\tilde{H}^1(\Omega_H))$, $p_s \in L^2(0,T,H^1(\Omega_B))$, $p_w \in C([0,T],L^2(\Omega_H))$, $\partial_t p \in L^2(0,T,(H^1(\Omega_H))') + L^{r/r-1}(\Omega_{T,H})$, $I_{\text{ion}u}(u,w)\,p \in L^{r/r-1}(\Omega_{T,H})$, and satisfying the following weak formulation*

$$\begin{aligned}
&\iint_{\Omega_{T,H}} -\beta c_m \partial_t p\phi_i + \iint_{\Omega_{T,H}} \mathbf{M}_{\text{i}}(x)\nabla p_i\cdot\nabla\phi_i + \iint_{\Omega_{T,H}} \beta I_{\text{ion}u}(u,w)p\phi_i \\
&\qquad - \iint_{\Omega_{T,H}} H_u(u,w)p_w\phi_i + \iint_{\Omega_{T,H}} \epsilon_1(u-u_d)\phi_i = 0,\\
&\iint_{\Omega_{T,H}} -\beta c_m \partial_t \phi_e - \iint_{\Omega_H} \mathbf{M}_{\text{e}}(x)\nabla p_e\cdot\nabla\phi_e + \iint_{\Omega_B} \mathbf{M}_{\text{s}}(x)\nabla p_s\cdot\nabla\phi_s \\
&\qquad + \iint_{\Omega_{T,H}} \beta I_{\text{ion}u}(u,w)p\phi_e + \iint_{\Omega_{T,H}} H_u(u,w)p_w\phi_e - \iint_{\Omega_{T,H}} \epsilon_1(u-u_d)\phi_e = 0,\\
&\iint_{\Omega_{T,H}} -\partial_t p_w\phi_w - H_w(u,w)p_w\phi_w + \beta I_{\text{ion}w}(u,w)p\phi_w = 0,
\end{aligned}$$

for all $\phi_i,\phi_e \in L^2(0,T,\tilde{H}^1(\Omega_H)))\cap L^r(\Omega_{T,H})$, $\phi_s \in L^2(0,T,H^1(\Omega_B))$ and $\phi_w \in C([0,T],L^2(\Omega_H))$.
Note that the semidiscrete Galerkin finite element formulation to the adjoint bidomain-bath model (4.5)-(4.6) reads as follows: For $t > 0$, find $p_i^h(t),p_e^h(t),p^h(t),p_s^h(t),p_w^h(t) \in V^h$ such that (with the standard

finite element notation for L^2 scalar products) one has

$$
\left\{
\begin{aligned}
&-\beta c_m \frac{d}{dt}(p^h(t),\phi^h)_{\Omega_H} + \big(\mathbf{M}_{\rm i}(x)\nabla p_i^h(t),\nabla\phi_i^h\big)_{\Omega_H} \\
&\qquad\qquad = \big(-\beta {I_{\rm ion}}_u^h\, p^h(t) + H_u^h\, p_w^h(t) - \epsilon_1(u^h(t)-u_d^h(t))\,,\,\phi_i^h\big)_{\Omega_H}, \\
&-\beta c_m \frac{d}{dt}(p^h(t),\phi_e^h)_{\Omega_H} - \big(\mathbf{M}_{\rm e}(x)\nabla p_e^h(t),\nabla\phi^h\big)_{\Omega_H} + \big(\mathbf{M}_{\rm s}(x)\nabla p_s^h(t),\nabla\phi_s^h\big)_{\Omega_B} \\
&\qquad\qquad = \big(-\beta {I_{\rm ion}}_u^h\, p^h(t) - H_u^h\, p_w^h(t) + \epsilon_1(u^h(t)-u_d^h(t))\,,\,\phi_e^h\big)_{\Omega_B} \\
&-\frac{d}{dt}(p_w^h(t),\varphi^h)_{\Omega_H} = (H_w^h\, p_w^h(t) - \beta {I_{\rm ion}}_w^h\, p^h(t),\varphi^h)_{\Omega_H},
\end{aligned}
\right. \tag{5.1}
$$

for all $\phi_i^h,\phi_e^h,\phi_s^h,\varphi^h\in V^h$. Additionally, we set $p^h(T)=\mathbb{P}_{V^h}(p_T)=0$ and $p_w^h(T)=\mathbb{P}_{V^h}(p_{w,T})=0$. Moreover, the backward Euler integration method is employed for the time discretization of (5.1) with time step $\Delta t=T/N$. This results in the following fully discrete method: for $t>0$, find $p_i^h(t),p_e^h(t),p_s^h(t),p^h(t)$, $p_w^h(t)\in V^h$ such that

$$
\big(p_i^h,p_e^h,p^h,p_s^h,p_w^h\big)(t,\boldsymbol{x}) = \sum_{n=1}^{N}\big(p_i^{h,n},p_e^{h,n},p^{h,n},p_s^{h,n},p_w^{h,n}\big)(\boldsymbol{x})\mathbb{1}_{((n-1)\Delta t,n\Delta t]}(t),
$$

satisfy the following system

$$
\left\{
\begin{aligned}
&-\beta c_m\big(\frac{p^{h,n}-p^{h,n-1}}{\Delta t},\phi_i^h\big)_{\Omega_H} + \big(\mathbf{M}_i(x)\nabla p_i^{h,n},\nabla\phi_i^h\big)_{\Omega_H} \\
&\qquad\qquad = \big(-\beta {I_{\rm ion}}_u^{h,n}\, p^{h,n} + H_u^{h,n}\, p_w^{h,n} - \epsilon_1(u^{h,n}-u_d^{h,n})\,,\,\phi_i^h\big)_{\Omega_H} \\
&-\beta c_m\big(\frac{p^{h,n}-p^{h,n-1}}{\Delta t},\phi_e^h\big)_{\Omega} - \big(\mathbf{M}_e(x)\nabla p_e^{h,n},\nabla\phi_e^h\big)_{\Omega_H} + \big(\mathbf{M}_{\rm s}(x)\nabla p_s^{h,n},\nabla\phi_s^h\big)_{\Omega_B} \\
&\qquad\qquad = \big(-\beta {I_{\rm ion}}_u^{h,n}\, p^{h,n} - H_u^{h,n}\, p_w^{h,n} + \epsilon_1(u^{h,n}-u_d^{h,n})\,,\,\phi_e^h\big)_{\Omega_H} \\
&-\big(\frac{p_w^{h,n}-p_w^{h,n-1}}{\Delta t},\varphi^h\big)_{\Omega_H} = (H_w^{h,n}\, p_w^{h,n} - \beta {I_{\rm ion}}_w^{h,n}\, p^{h,n},\varphi^h)_{\Omega_H},
\end{aligned}
\right. \tag{5.2}
$$

for all $\phi_i^h,\phi_e^h,\phi_s^h,\varphi^h\in V^h$ and for all $n\in\{1,\dots,N\}$.

Our second main result is

THEOREM 5.1. *Assume that* (2.1)-(2.4) *and* (4.7) *hold. Then the finite element solution* $\boldsymbol{p}_h=\big(p_i^h,p_e^h,p^h,p_s^h,p_w^h\big)$, *generated by* (5.2)*, converges along a subsequence to* $\boldsymbol{p}=(p_i,p_e,p,p_s,p_w)$ *as* $h\to 0$*, where* $\boldsymbol{p}$ *is a weak solution of the system* (4.5)-(4.6)*. Moreover the weak solution is unique.*

Now, we establish existence and uniqueness of solutions (proof of Theorem 5.1) to the finite element scheme, and show that it converges to a weak solution of the adjoint bidomain-bath model. The convergence proof is based on deriving the series of a priori estimates and using a general L^1 compactness criterion. Let us indicate its main steps.

5.1. A priori estimates. Assuming that there exists a discrete finite element solution $\boldsymbol{p}_h=\big(p_i^h,p_e^h,p^h,p_s^h,p_w^h\big)$ to the above problems (this can be obtained exactly as in the proof of Proposition 3.1), we derive estimates that are uniform in $h>0$. We substitute $\phi_i^h=p_i^{h,n}$, $\phi_e^h=-p_e^{h,n}$, $\phi_s^h=p_e^{h,n}$, and $\varphi^h=p_w^{h,n}$ in (5.2), respectively. Then integrating over $(0,T)$, using Young and Gronwall inequalities, we get

$$
\begin{aligned}
&\big\|p^h\big\|_{L^\infty(0,T;L^2(\Omega_H))} + \big\|p_w^h\big\|_{L^\infty(0,T;L^2(\Omega_H))} + \Big\|{I_{\rm ion}}_u^h\,\big|p^h\big|^2\Big\|_{L^1(\Omega_{T,H})} \le c_1, \\
&\sum_{j=i,e}\big\|\nabla p_j^h\big\|_{L^2(0,T;L^2(\Omega_H))} + \big\|\nabla p_s^h\big\|_{L^2(0,T;L^2(\Omega_B))} \le c_2,
\end{aligned} \tag{5.3}
$$

for some constants $c_1, c_2 > 0$ not depending on h. Using this and an application of Young inequality, we get

$$
\begin{aligned}
\left\| I_{\mathrm{ion}_u}^h p^h \right\|^{r/r-1}_{L^{r/r-1}(\Omega_{T,H})} &\leq c_3 \iint_{\Omega_{T,H}} \left| u^{h^{r-2}} p^h \right|^{r/r-1} \\
&\leq c_3 \iint_{\Omega_{T,H}} \left| u^{h^{(r-2)/2}} p^h \right| \left| u^{h^{((r+1)(r-2))/2}} p^h \right|^{1/r-1} \\
&\leq \frac{c_1\, c_3}{2} + \frac{c_3}{2} \iint_{\Omega_{T,H}} \left| u^{h^{((r+1)(r-2))/2}} p^h \right|^{2/r-1} \\
&\leq \frac{c_1\, c_3}{2} + c_4 \iint_{\Omega_{T,H}} \left| u^h \right|^r + c_5 \iint_{\Omega_{T,H}} \left| u^{h^{(r-2)}} \left| p^h \right|^2 \right| \\
&\leq c_6,
\end{aligned}
\tag{5.4}
$$

for some constant $c_3, c_4, c_5, c_6 > 0$ not depending on h. This implies that the $L^{r/r-1}$ uniform bound of $I_{\mathrm{ion}_u}^h p^h$.

5.2. L^1-Space and time translation estimates. First, we introduce $\bar{p}^h$ and $\bar{p}_w^h$ the piecewise affine in t functions in $W^{1,\infty}([0,T]; V^h)$ interpolating the states $(u^{h,n})_{n=0..N} \subset V^h$ and $(w^h)_{n=0..N} \subset V^h$ at the points $(n\Delta t)_{n=0..N}$. Then we have

$$
\begin{cases}
-\beta c_m \partial_t \bar{p}^h - \nabla \cdot (\mathbf{M}_i(x) \nabla p_i^h) + \beta I_{\mathrm{ion}\, u}(u,w) p^h - H_u(u,w) p_w^h + \epsilon_1 (u - u_d) = 0 & \text{in } \Omega_{T,H}\ , \\
-\beta c_m \partial_t \bar{p}^h + \nabla \cdot (\mathbf{M}_e(x) \nabla p_e^h) + \beta I_{\mathrm{ion}\, u}(u,w) p^h + H_u(u,v) p_w^h - \epsilon_1 (u - u_d) = 0 & \text{in } \Omega_{T,H}\ , \\
-\nabla \cdot (\mathbf{M}_{\mathrm{s}}(x) \nabla p_s^h) = 0 & \text{in } \Omega_{T,B}\ , \\
-\partial_t \bar{p}_w^h - H_w(u,w) p_w^h + I_{\mathrm{ion}\, w}(u,v) p^h = 0 & \text{in } \Omega_{T,H}\ ,
\end{cases}
\tag{5.5}
$$

Now, we prove that the family $(p^h, p_w^h)_h$ of discrete solutions constructed in Subsection 5.1 is relatively compact in $L^1(\Omega_{T,H})$. With this aim, we will use the following lemma.

LEMMA 5.2. *For all $\Omega'_H \subset\subset \Omega_H$ and $\nu, \tau > 0$ small enough, there exist functions $\mathcal{C}_1$ and $\mathcal{C}_2$ not depending on h such that*

$$
\sup_{|\boldsymbol{r}| \leq \nu} \iint_{\Omega'_H \times (0,T)} \left| p^h(t, x + \boldsymbol{r}) - p^h(t,x) \right| \, dx\, dt \leq \mathcal{C}_1(\nu),
\tag{5.6}
$$

and

$$
I^h := \int_0^{+\infty} \int_{\Omega'_H} |\bar{p}^h(t+\tau', x) - \bar{p}^h(t,x)| \, dx dt \leq \mathcal{C}_2(\tau),
\tag{5.7}
$$

for all $\boldsymbol{r} \in \mathbb{R}^3$ and all $\tau' \in (0, \tau]$, where $\mathcal{C}_1(\nu) \to 0$ and $\mathcal{C}_2(\tau) \to 0$ as $\nu, \tau \to 0$.

Proof. Note that it is easy to prove (5.6) by exploiting (5.3) and using the same lines as in the of proof of (3.16). Throughout the next proof, C will denote a generic constant independent of h and δ.

Now we adapt the idea of Kruzhkov Lemma (see for e.g. [19]) to our discrete solution p^h to prove a uniform estimate of the time translates (5.7) of $(\bar{p}^h)_h$. Next, we fix h and $\tau' \in (0, \tau]$, and we set

$$
T^h p^h(t, \cdot) = \bar{p}^h(t + \tau', \cdot) - \bar{p}^h(t, \cdot).
$$

Observe that $T^h p^h(t, \cdot) \equiv 0$ for large t. We take a standard family $(\rho_\delta)_\delta$ of mollifiers on $\mathbb{R}^3$ ($\rho_\delta(x) := \delta^{-3} \rho(x/\delta)$, where ρ is a Lipschitz continuous, nonnegative function supported in the unit ball of $\mathbb{R}^3$, and $\int_{\mathbb{R}^3} \rho(x)\, dx = 1$). It is easy to see that

$$
|\nabla \rho_\delta| \leq \frac{C}{\delta^4}.
$$

For all $t > 0$, we define the function $\varphi(t,\cdot) : \mathbb{R}^3 \longrightarrow \mathbb{R}$ by $\varphi(t) := \rho_\delta * (\operatorname{sign} T^h p^h(t) \mathbb{1}_{\Omega'_H})$. Note that the function $\varphi(t) \equiv 0$ on the set $\left\{x \in \Omega_H \,\middle|\, \operatorname{dist}(x, \overline{\Omega_H}) \geq \delta + h\right\}$, for all t. This implies that for all sufficiently small h and δ, the support of $\varphi(t)$ is included in some domain Ω''_H, $\Omega''_H \subset \Omega_H$.

Now, multiplying the first equation in (5.5) by $\varphi(t)$, integrating in t on $[s, s+\tau']$, making the integration over Ω'_H and finally, integrating the obtained equality in s over $\mathbb{R}^+$, we get

(5.8)
$$I^h_\delta(\tau') := \int_0^{+\infty} \int_{\Omega'_H} \varphi(s) T^h p^h(s)\, dxds = \int_0^{+\infty} \int_s^{s+\tau'} \int_{\Omega_H} \varphi(t) \Big(\nabla \cdot (\mathbf{M}_i(x) \nabla p^h_i) + \beta I_{\mathrm{ion}\, u}(u,w) p^h - H_u(u,w) p^h_w + \epsilon_1 (u - u_d) \Big)\, dxdtds.$$

Denote $Q''_{T,H} = (0,T) \times \Omega''_H$. An application of the Fubini theorem, we obtain

$$I^h_\delta(\tau') \leq C\tau' \left(\| \nabla p^h_i \|_{L^1(Q''_{T,H})} \| \nabla \varphi \|_{L^\infty(Q''_{T,H})} \;+\; \|\varphi\|_{L^\infty(Q''_{T,H})} \|f^h\|_{L^1(Q''_{T,H})} \right),$$

where

$$Q''_{T,H} = (0,T) \times \Omega''_H \text{ and } f^h = \beta I_{\mathrm{ion}\, u}(u,w) p^h - H_u(u,w) p^h_w + \epsilon_1 (u - u_d).$$

Now we use the $L^1_{loc}([0,T] \times \Omega_H)$ bounds (5.3)-(5.4) on $(\nabla p^h_i)_h$,$(f^h)_h$, the bounds $|\varphi(t,\cdot)| \leq 1$, $|\nabla \varphi(t,\cdot)| \leq C/\delta^4$, to get the estimate (for all h and δ small enough, uniformly in h)

$$I^h_\delta(\tau') \leq C\tau'(1 + \delta^{-4}). \tag{5.9}$$

Moreover, note that

(5.10)
$$\int_0^{+\infty} \int_{\Omega_H} |\bar{p}^h(t+\tau', x) - \bar{p}^h(t,x)|\, dxdt - I^h_\delta(\tau') = \int_0^{+\infty} \int_{\Omega_H} \big(|T^h p^h(t,x)| - T^h p^h(t,x) \varphi(t,x) \big)\, dxdt.$$

Next, we set $S'_\delta := \left\{x \in \mathbb{R}^3 \,\middle|\, \operatorname{dist}(x, \partial\Omega'_H) < \delta\right\}$. Observe that $S'_\delta \subset \Omega''_H \Subset \Omega_H$ for all δ small enough. By the result (5.6) and the Frechet-Kolmogorov theorem, the family $\left(\int_0^{+\infty} |T^h p^h(t,\cdot)| dt \right)_h$ is relatively compact in $L^1_{loc}(\Omega_H)$. This implies that these functions are equi-integrable on Ω''_H, so that

$$\int_0^{+\infty} \int_{S'_\delta} |T^h p^h(t,x)| dxdt \leq \hat{\mathcal{C}}_1(\delta) \text{ uniformly in } h, \text{ with } \lim_{\delta \to 0} \hat{\mathcal{C}}_1(\delta) = 0.$$

Now we use the definition of φ and formula (5.10) to deduce

$$\begin{aligned} &\left| \int_0^{+\infty} \int_{\Omega_H} |\bar{p}^h(t+\tau', x) - \bar{p}^h(t,x)|\, dxdt - I^h_\delta(\tau) \right| \\ &\quad \leq 4 \int_0^{+\infty} \int_{S'_\delta} |T^h p^h(t,x)| dxdt + \int_0^{+\infty} \int_{\Omega'_H \setminus S'_\delta} \Big| |T^h p^h(t,x)| - T^h p^h(t,x) (\rho_\delta * \operatorname{sign} T^h p^h(t))(x) \Big|\, dxdt. \end{aligned}$$

By the properties of ρ_δ, we deduce

$$\begin{aligned} &\left| \int_0^{+\infty} \int_{\Omega_H} |\bar{p}^h(t+\tau', x) - \bar{p}^h(t,x)|\, dxdt - I^h_\delta(\tau) \right| \\ &\quad \leq 4\hat{\mathcal{C}}_1(\delta) + \int_0^{+\infty} \int_{\Omega'_H \setminus S'_\delta} \int_{\mathbb{R}^l} \rho_\delta(x-y) \Big| |T^h p^h(t,x)| - T^h p^h(t,x) \operatorname{sign} T^h p^h(t,y) \Big|\, dydxdt, \end{aligned}$$

where $\lim_{\delta\to 0}\hat{\mathcal{C}}_2(\delta)=0$ uniformly in h. Now note the key inequality:

$$\forall a,b\in\mathbb{R}\qquad \big||a|-a\,\mathrm{sign}\,b\big|\le 2\,|a-b|.$$

Next we set $\sigma:=(x-y)/\delta$ and we use the inequality $\big||a|-a\,\mathrm{sign}\,b\big|\le 2\,|a-b|$ for all $a,b\in\mathbb{R}$, to get

$$\begin{aligned}
&\left|\int_0^{+\infty}\!\!\int_{\Omega_H}|\bar{p}^h(t+\tau',x)-\bar{p}^h(t,x)|\,dxdt-I^h_\delta(\tau)\right|\\
&\quad\le\ 4\hat{\mathcal{C}_1}(\delta)\ +\ 2\int_0^{+\infty}\!\!\int_{\Omega'}\int_{\mathbb{R}^3}\rho_\delta(x-y)|T^hp^h(t,x)-T^hp^h(t,y)|\,dydxdt\\
&\quad\le 4\hat{\mathcal{C}_1}(\delta)\ +\ 2\int_{\mathbb{R}^3}\rho(\sigma)\int_0^{+\infty}\!\!\int_{\Omega'_H}|\bar{p}^h(t,x)-\bar{p}^h(t,x-\delta\sigma)|\,dxdt\,d\sigma\\
&\quad\le\ 4\hat{\mathcal{C}_1}(\delta)+2\hat{\mathcal{C}_2}(\delta),
\end{aligned}\tag{5.11}$$

where $\hat{\mathcal{C}_2}(\cdot)$ is the modulus of continuity controlling the space translates of $\bar{p}^h$ in Ω'_H (this can be chosen independent of h). Combining (5.9) with (5.11), we conclude that the function, the inequality in I^h (5.7),

$$\mathcal{C}_2(\tau):=\inf_{\delta>0}C\left\{\ \tau\,(1+\delta^{-4})+4\hat{\mathcal{C}_2}(\delta)+2\hat{\mathcal{C}_2}(\delta)\ \right\}$$

tends to 0 as $\tau\to 0$. This concludes the proof of Lemma 5.2. □

By the Riesz-Frechet-Kolmogorov compactness criterion, the relative compactness of $(\bar{p}^h)_h$ and $(\bar{p}^h_w)_h$ in $L^1_{loc}([0,T]\times\Omega_H)$ is a consequence of Lemma 5.2. In order to conclude, it suffices to show that $\|p^h-\bar{p}^h\|_{L^1(\Omega')}\to 0$ and $\|p^h_w-\bar{p}^h_w\|_{L^1(\Omega')}\to 0$ as $h\to 0$ but this can be shown exactly as in Lemma 3.2, so we omit the details.

With the help of a compactness tool inspired by Lemma 3.2, we justify that the solution (p^h,p^h_w) is relatively compact in $L^1(\Omega_H)$. Moreover, using the Sobolev embedding of $L^2(0,T;H^1(\Omega_H))$ into $L^2(0,T;L^6(\Omega_H))$ and the space interpolation with $L^\infty(0,T;L^2(\Omega_H))$, we find a uniform $L^{10/3}(\Omega_H)$ bound on p^h. The consequence of this and the strong convergence of p^h, (5.3) and (5.4) is the following convergence (at the cost of extracting subsequences, which we do not bother to relabel), we can assume there exist limit functions (p,p_i,p_e,p_s,p_w) such that,

$$\begin{cases}
p^h\to p \text{ almost everywhere in } \Omega_{H,T} \text{ and strongly in } L^\rho \text{ for } 1\le\rho<\frac{10}{3},\\
p^h_w\to p_w \text{ almost everywhere in } \Omega_{H,T} \text{ strongly in } L^2(\Omega_{T,H}),\\
p^h\rightharpoonup p \text{ weakly in } L^2(0,T;H^1(\Omega_H)),\\
p^h_i\rightharpoonup p_i \text{ weakly in } L^2(0,T;\tilde{H}^1(\Omega_H)),\\
p^h_e\rightharpoonup p_e \text{ weakly in } L^2(0,T;\tilde{H}^1(\Omega_H)),\\
p^h_s\rightharpoonup p_s \text{ weakly in } L^2(0,T;H^1(\Omega_B)).
\end{cases}\tag{5.12}$$

Next, using (5.12) sending h to 0 in the following weak formulation delivers the existence of a weak global solution

$$\begin{aligned}
&\iint_{\Omega_{T,H}}-\beta c_m\partial_t\bar{p}^h\phi_i+\iint_{\Omega_{T,H}}\mathbf{M_i}(x)\nabla p^h_i\cdot\nabla\phi_i+\iint_{\Omega_{T,H}}\beta I_{\mathrm{ion}_u}{}^h p^h\phi_i\\
&\qquad-\iint_{\Omega_{T,H}}H^h_up^h_w\phi_i+\iint_{\Omega_{T,H}}\epsilon_1(u^h-u^h_d)\phi_i=0,\\
&\iint_{\Omega_{T,H}}-\beta c_m\partial_t\bar{p}^h\phi_e-\iint_{\Omega_H}\mathbf{M_e}(x)\nabla p^h_e\cdot\nabla\phi_e+\iint_{\Omega_B}\mathbf{M_s}(x)\nabla p^h_s\cdot\nabla\phi_s\\
&\qquad+\iint_{\Omega_{T,H}}\beta I_{\mathrm{ion}_u}{}^h\,p\,\phi_e+\iint_{\Omega_{T,H}}H^h_up^h_w\phi_e-\iint_{\Omega_{T,H}}\epsilon_1(u^h-u^h_d)\phi_e=0\\
&\iint_{\Omega_{T,H}}-\partial_t\bar{p}^h_w\phi_w-H^h_wp^h_w\phi_w+\beta I_{\mathrm{ion}_w}{}^h p^h\phi_w=0,
\end{aligned}\tag{5.13}$$

for all $\phi_i, \phi_e \in L^2(0,T,\tilde{H}^1(\Omega_H)) \cap L^r(\Omega_{T,H})$, $\phi_s \in L^2(0,T,H^1(\Omega_B))$ and $\phi_w \in C([0,T],L^2(\Omega_H))$.

Finally, the uniqueness of the adjoint solution can be obtained exactly by using the technique in Theorem 3.5.

6. Numerical approach. In this subsection we demonstrate the numerical procedure to solve the optimization problem (4.1) subject to the complete bidomain-bath equations. In this regard, the brief overview of the numerical discretization of primal problem is given. We use the elliptic-parabolic form of the bidomain-bath equations (1.7) for the computer implementation.

In our approach, the elliptic system on the tissue domain (u_e) and on bath domain (u_s) is solved monolithically. For this purpose we define v as the extracellular potential on $\Omega_H \cup \Omega_B$, i.e.:

$$v = \begin{cases} u_s & \text{in } \Omega_B \\ u_e & \text{in } \Omega_H \end{cases}$$

and the similar way we can define the global conductivity tensor as follows.

$$\bar{\sigma} = \begin{cases} \mathbf{M}_s(x) & \text{in } \Omega_B \\ (\mathbf{M}_i(x) + \mathbf{M}_e(x)) & \text{in } \Omega_H \end{cases}$$

We use the piecewise linear finite element method for the spatial discretization of partial differential equations in the primal problem. After the space discretization we obtain the following ordinary differential equations.

Here, the approximate solutions of the vectors $\mathbf{u}$, $\mathbf{v}$ and $\mathbf{w}$ are expressed in the form $\mathbf{v}(t) = \sum_{i=1}^{M+N} v_i(t)\omega_i$, $\mathbf{u}(t) = \sum_{i=1}^{N} u_i(t)\omega_i$ and $\mathbf{w}(t) = \sum_{i=1}^{N} w_i(t)\omega_i$, respectively, where $\{\omega_i\}_{i=1}^{M}$ and $\{\omega_i\}_{i=1}^{N}$ denote the basis functions. In this N and M denote the number of nodal points at the tissue domain and the bath domain respectively. This semi-discretization in space results in the following matrix representation of the differential algebraic system.

$$\mathbf{A_{ie}}\mathbf{v} + R_H\mathbf{A_i}\mathbf{u} = \mathcal{I}_s \tag{6.1}$$

$$\mathbf{M}\frac{\partial \mathbf{u}}{\partial t} = -\mathbf{A_i}\mathbf{u} - R_B\mathbf{A_i}\mathbf{v} - I_{\text{ion}}(\mathbf{u},\mathbf{w}) + \mathcal{I}_{tr} \tag{6.2}$$

$$\mathbf{M}\frac{\partial \mathbf{w}}{\partial t} = \mathbf{G}(\mathbf{u},\mathbf{w}), \tag{6.3}$$

together with initial conditions for $\mathbf{u}$ and $\mathbf{w}$, where $\mathbf{A_{ie}} = \{\langle(\sigma_i+\sigma_e)\nabla\omega_i, \nabla\omega_j\rangle\}_{i,j=1}^{M+N}$ and $\mathbf{A_i} = \{\langle\sigma_i\nabla\omega_i, \nabla\omega_j\rangle\}_{i,j=1}^{N}$ are the stiffness matrices, $\mathbf{M} = \{\langle\omega_i,\omega_j\rangle\}_{i,j=1}^{N}$ is the mass matrix. The vectors $\mathcal{I}_s, \mathcal{I}_{tr}$ are defined by $\mathcal{I}_s = \{\langle(\chi_{\Gamma_1}I_e - \chi_{\Gamma_2}I_e), \omega_j\rangle\}_{j=1}^{M_\Gamma}$ and $\mathcal{I}_{tr} = \{\langle I_{tr}, \omega_j\rangle\}_{j=1}^{N}$, respectively. Here the R_H and R_B represent the restriction operator from the tissue domain to the integrated domain and from the integrated domain to the tissue domain respectively. The expressions $I_{\text{ion}}(\mathbf{u},\mathbf{w})$ and $\mathbf{G}(\mathbf{u},\mathbf{w})$ are defined by

$$I_{\text{ion}}(\mathbf{u},\mathbf{w}) = \{\langle I_{\text{ion}}\left(\sum_{i=0}^{N} u_i\omega_i, \sum_{i=0}^{N} w_i\omega_i\right), \omega_j\rangle\}_{j=1}^{N},$$

$$\mathbf{G}(\mathbf{u},\mathbf{w}) = \{\langle G\left(\sum_{i=0}^{N} u_i\omega_i, \sum_{i=0}^{N} w_i\omega_i\right), \omega_j\rangle\}_{j=1}^{N}.$$

REMARK 6.1. *We point out that the boundary control in the bidomain-bath model* (1.7) *is transformed as a locally distributed control in the discretized equations due to our computational approach. In fact, it appears as a line electrodes on the whole domain in our 2D computations.*

We use the backward Euler time stepping scheme for the time discretization of the ODEs Eqs. (6.2)-(6.3). In our computational approach, those semi discretized ODEs are solved as a coupled system which

can be expressed in the following matrix representation.

$$\mathcal{M}\frac{\partial \mathbf{x}}{\partial t} = \mathcal{F}(\mathbf{v}, \mathbf{u}, \mathbf{w}), \qquad \mathbf{x}(t^0) = \mathbf{x^0}. \tag{6.4}$$

where

$$\mathcal{M} = \begin{pmatrix} \mathbf{M} & 0 \\ 0 & \mathbf{M} \end{pmatrix}, \quad \mathbf{x} = \begin{pmatrix} \mathbf{u} \\ \mathbf{w} \end{pmatrix}, \tag{6.5}$$

$$\mathcal{F}(\mathbf{v}, \mathbf{u}, \mathbf{w}) = \begin{pmatrix} -\mathbf{A_i}\mathbf{v} - R_B\mathbf{A_i}\mathbf{u} - I_{\text{ion}}(\mathbf{v}, \mathbf{w}) + \mathcal{I}_{tr} \\ \mathbf{G}(\mathbf{v}, \mathbf{w}) \end{pmatrix} \tag{6.6}$$

The backward Euler time discretization of the Eq. (6.4) leads to system of algebraic equations as follows.

$$\mathcal{M}\mathbf{x}^n = \mathcal{M}\mathbf{x}^{n-1} + \Delta t\mathcal{F}(\mathbf{v}^n, \mathbf{u}^n, \mathbf{w}^n) \tag{6.7}$$

Here we give the essential steps to the solving primal problem, see [14] for complete algorithm and parallel implementation issues. At every time step, first we solve the discretized elliptic system (6.1) by using the Conjugate Gradient(CG) method with AMG preconditioner, see [6]. Note that we use the stabilized saddle point approach, see for more details [13] to incorporate the zero mean condition into the solution procedure. In the second step, the fully discretized PDEs (6.7) are solved by the Newton's method. In each step of Newton's method, the linearized subproblem is solved by a standard BiCGSTAB method with Jacobi preconditioning.

Analogously, we follow the piecewise linear finite element method for the spatial discretization and backward Euler time stepping scheme for the time discretization of the dual equations which needs to be solved backward in time. One can obtain the similar matrix representation system as in Eqs. (6.1)-(6.3).

The complete optimality system is solved by the Newton-CG optimization algorithm, see for complete details in [14]. In our computations, the line search algorithm is based on an Armijo type condition. The termination of the optimization algorithm is based on the following criteria:

$$\left\|\nabla J(u^k, \mathcal{I}^k)\right\|_{L^2} \leq 10^{-3} \cdot \left|J(u^k, \mathcal{I}^k)\right| \text{ or } \left|J(u^k, \mathcal{I}^k) - J(u^{k-1}, \mathcal{I}^{k-1})\right| \leq 10^{-4} \tag{6.8}$$

If this condition was not satisfied within a prescribed number of 12 iterations, the algorithm is terminated. We developed a complete optimization code based on the public domain FEM software package DUNE [4]. Moreover, we employ the same spatial discretization technique for the linearized primal and dual equations which are part of the Newton's optimization algorithm, see [14] for more algorithmic details.

7. Numerical results. The numerical results of the optimal control to termination of reentry waves are presented in this section. The computational domain of the integrated geometry is $\Omega := \Omega_H \cup \Omega_B = [-0.15, 3.3] \times [-0.15, 2.19] \in \mathbb{R}^2$ and it consists of 230×156 uniform quadrilateral elements. The embedded cardiac tissue domain size is $\Omega_H = [0, 3.15] \times [0, 2.04] \in \mathbb{R}^2$ and a 210×136 uniform quadrilateral spatial grid is used. During the simulations, we fix the time step length $\Delta t = 0.02\ msec.$ The computational domain and various relevant subdomains are depicted in Figure 1 and we used the parameters from [14] for the current bidoman-bath model with the consideration of Mitchel-Schaffer model as the ionic model.

We followed a standard $S1-S2$ stimulation protocol to induce the reentry at the computational domain, for more details see [14]. Here the initial solution for the u_0 and w_0 is considered as a resting state solution at the complete tissue domain. In this framework, the brief overview of the three temporal horizons is depicted in Figure 2 to induce the reentry, applied shock strength duration and post shock simulation duration. The initial solution of the extracellular potential on the integrated domain, the transmembrane voltage and the gating state solution is depicted in Figure 3 at simulation time of 710 msec. In our simulations, the direct simulation was carried out until time $t = 3200$ msec to ensure that the induced reentry is maintained for a prolonged period of time. This can be attributed to the cardiac arrhythmia in the real life situation. In this test case the initial guess of the control for optimization algorithm is taken as $I_s(t) = 1$ mA/cm^3.

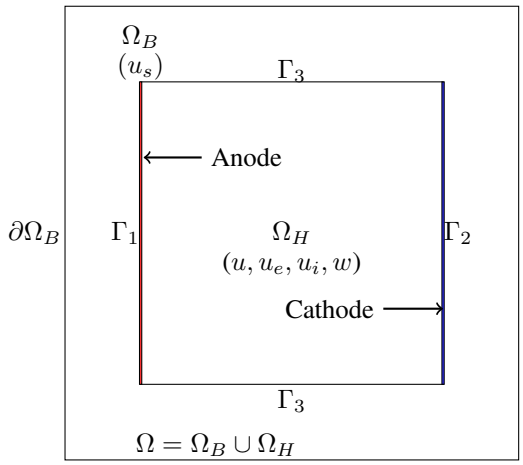

FIG. 1. *The schematic view of the computational domain setup with stimulation boundaries.*

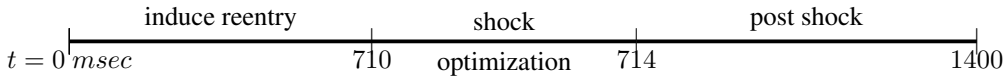

FIG. 2. *Different time horizons considered in the computations.*

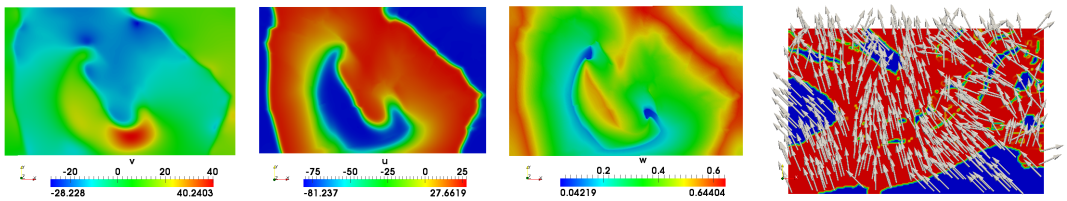

FIG. 3. *The initial solution of state variables v, u and w at time 710 msec. The last figure represents the glyph of the fiber directions $a_l(x)$.*

The conductivity values were chosen to arrive at physiologically relevant conduction velocities of 0.61 m/s and 0.38 m/s along and transverse to the principal fiber axes, respectively, and to keep anisotropy ratios within the range of values reported in experimental studies [23]. A rule-based method was used to impose fiber orientations using fiber angles of -60° and +60° at the endocardial and epicardial surfaces, respectively, and a smooth linear variation of fiber angles as a function of depth in between. The glyph of the fiber directions $a_l(\mathbf{x})$ at the cardiac tissue is shown in last figure of Figure 3 which are used to compute the anisotropic conductivity tensor values accordingly Eq (1.2).

The presented numerical results were computed on a Linux cluster consisting of ten nodes where each node consists of 2 quad-core AMD Opteron processors 8356 clocked at 2.3 GHz and equipped with 1TB RAM. All presented results are based on the parallel Newton-CG algorithms using up to 64 cores.

7.1. Termination of reentry waves. In this section we demonstrate the feasibility of optimal control approach to the termination of reentry waves by utilizing less applied current. To achieve successful defibrillation, the desired trajectory of the transmembrane potential (v_d) needs to be specified. For the realization of this, a solution of the primal problem was generated using a prescribed time course (4 msec) of a stimulation current, $I_s(t) = 6$ mA/cm^3. The computed desired trajectory ensures that optimized states attain a steady state during the post shock period.

In this test case, the optimal control strategy will compute the suitable optimal control for termination

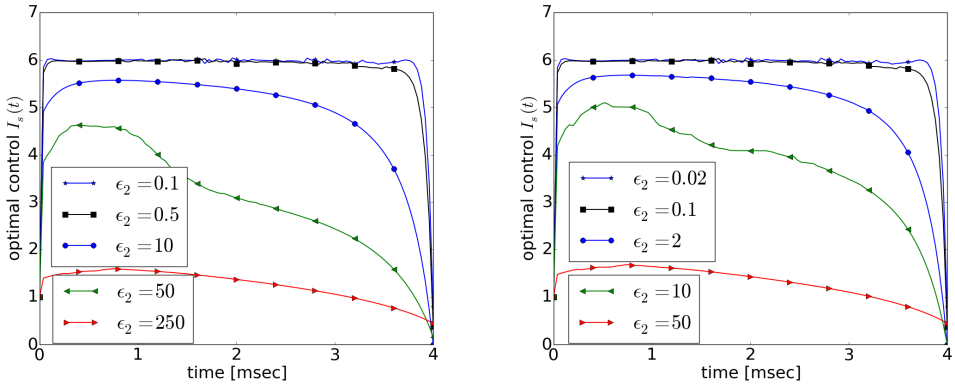

FIG. 4. *The optimal control solution for different values of ϵ_1 and ϵ_2 parameters.*

of reentry waves by proper adjustment of weights at the observation (ϵ_1) and at the cost (ϵ_2) in the cost functional (4.1). In the left hand side of Figure 4, the weight at the observation domain is fixed ϵ_1 = 0.5 and varied the weight of the cost ϵ_2 = 0.1, 0.5, 10, 50 and 250. We observed that successful defibrillation is observed during the post shock simulations except for $\epsilon_2 = 250$. By reducing the value of ϵ_2 the successful defibrillation is achieved for this test case. With the values of $\epsilon_2 = 0.1$ and 0.5, the optimal control trajectory is very close to the adhoc strategy control value which is used to compute the desired trajectory. In the right hand side of Figure 4, the weight of the observation is fixed at ϵ_1 = 0.1 and analyzed the effect of varying the weight of the cost value ϵ_2 = 0.02, 0.1, 2, 10 and 50. Here we can observe that the optimal control trajectories for both cases predict in the similar way. This test case clearly reflects that the optimal control only depends on the ratio of $\frac{\epsilon_2}{\epsilon_1}$. In the optimization procedure ϵ_1 acts as a scaling of the adjoint variables (p_s, p_e, p_i, p_w). For fixed ϵ_1, the weight ϵ_2 describes the relative weight of the cost control I_e.

The L^2-norm of the gradient of the cost functional is shown in Figure 5 for ϵ_1 = 0.5 and different values of the weight of the cost ϵ_2 = 0.1, 0.5, 10, 50 and 250 where the norm of the gradient value is depicted on log scale for better reading at the last iterations of optimization algorithm. We can observe that the norm of the gradient value is reduced rapidly during the first iterations of optimization algorithm which is about 4739.5. Then the reduction is very small at the last iterations and the smallest gradient value is $8E{-}3$.

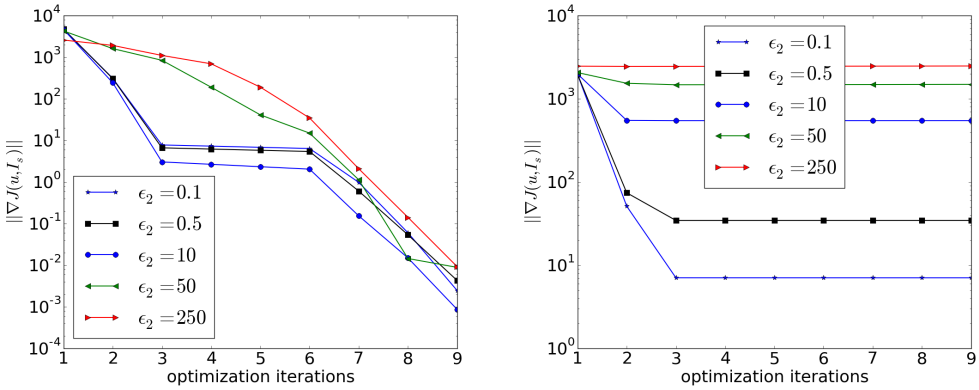

FIG. 5. *The optimal control solution for different values of ϵ_1 and ϵ_2 parameters.*

The corresponding minimization value is depicted in right hand side of Figure 5. We can observe that for smaller values of ϵ_2, the cost functional obtained has smallest minimization value which is 7.05.

We remark that the Newton-CG optimization algorithm accept the step length 0.25 at the beginning of optimization algorithm as contrast to the initial step length 1.0. At the end of the optimization iterations, it accepts the full step length. Due to this phenomena we observed that the superlinear convergence is achieved at the end of the optimization iterations.

The optimal state solution of the transmembrane voltage is depicted in Figure 6 at different time instances during the shock period. The well known virtual electrode polarization (VEP) starts to appear from time t= 710.08, which can clearly see at first panel in Figure 6 The VEP rises sharply in some parts of the computational domain at the beginning of shock period and then it appear all over the tissue in both excitable gap as well as in depolarized regions at the end of shock period which effectively blocked the further propagation of the spiral wave.

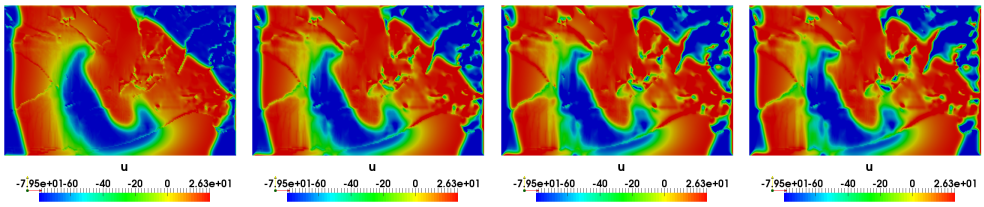

FIG. 6. *The optimal state solution of transmembrane voltage u during the shock period at times t= 710.08, 712.0, 713.04 and 713.80 msecs respectively.*

The 2D colored plots of uncontrolled transmembrane voltage solution is shown in Figure 7 for different time instances. Here we can observe that initially the spiral wave evolve spatially and transform to single spiral wave at time 1171.

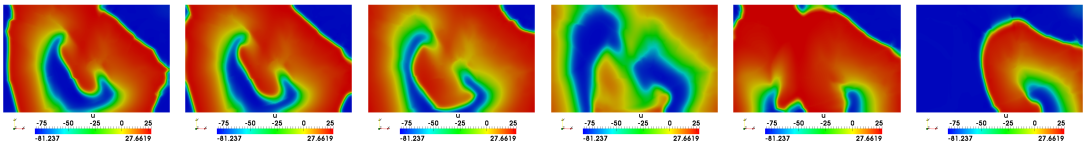

FIG. 7. *The uncontrolled solution of transmembrane voltage u at times t= 714, 722.53, 752.53, 812.53, 961.53 and 1171 msecs respectively.*

The spatio-temporal evolution of the reentrant activation for controlled solution of the transmembrane solution is depicted in Figure 8. At simulation time 714 msec, the appearance of virtual electrodes presents at the whole tissue domain and such effect slowly disappeared at time 751.73 msec. Due to the less excitable gap as well as the depolarized regions effectively blocked the further propagation of the spiral wave. At time 1182 msec the spiral wave disappeared completely from the computational domain.

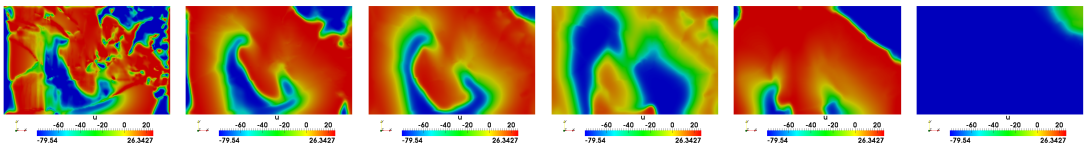

FIG. 8. *The controlled state solution of transmembrane voltage u at times t= 714, 721.73, 751.73, 811.73, 961.73 and 1171 msecs respectively.*

7.2. Convergence test with different mesh refinement levels. In this test case the convergence of the optimal control approach is presented with respect to the different grid hierarchies. The initial coarse grid dimension is 230×156 is fixed for the whole domain and corresponding the initial mesh for the tissue

domain is 210×136. The subsequent finer grid meshes are generated by taking the uniform refinement on the initial coarse grid level which refines at both(whole domain and the tissue domain) spatial grid domains.

Grid dimension	$\|u(x,t) - u_d(x,t)\|^2$	CG iter	Newton iter
230×156	458.03	9	8
460×312	453.69	10	8
920×624	447.41	11	8
1840×1248	445.49	11	8
3680×2496	444.63	11	8

The numerical convergence history of the optimization algorithm for different mesh levels is shown in Table 7.2. The first column shows the grid dimension in x- and y-direction of the whole domain. Here the finest grid level comprises of 9,169,371 degrees of freedom (DOFs) on the whole domain and the 27,508,113 DOFs at the tissue domain. The second column represents the L^2-norm of the computed optimized solution and desired solution of the transmembrane potential for different grid sizes.

The third column shows an average inner CG iterations of the optimization algorithm and the last column represents the total Newton iterations to terminate the optimization algorithm. This evident that the optimization algorithm robust with respect to the finer meshes. Now we turn to the discussion on computational times. The initial coarse grid optimization computation took approximately 2 hours 4 min of CPU time on 4 cores and the finest grid level computation has taken 38 hours 24 min of CPU time on 64 cores. We observed that the optimization algorithm converged superlinearly at all these mesh sizes.

FIG. 9. *The optimal control with respect to the different mesh sizes.*

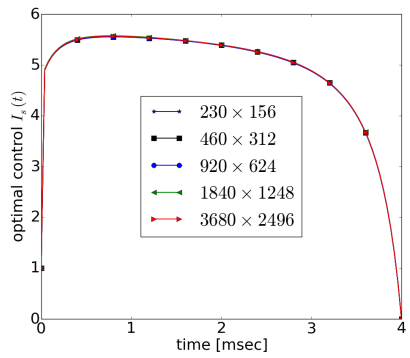

The optimal control solution of the different mesh refinement levels is depicted in Figure 9. Here we can observe that all mesh level solutions has good agreement over the time horizon. The total current is 19.593 mA/cm^3, 19.602 mA/cm^3, 19.610 mA/cm^3, 19.613 mA/cm^3 and 19.615 mA/cm^3 correspondingly for the different mesh levels shown in Table 7.2.

The convergence proof uses two ingredients of interest for various applications, namely the discrete Sobolev embedding inequalities with general boundary conditions and a space-time L1 compactness argument that mimics the compactness lemma due to S.N. Kruzhkov

8. Conclusion. In this paper, we presented the numerical analysis of a finite element scheme for the optimal control of bidomain-bath model in cardiac electrophysiology. In this regard, first we proved the existence and uniqueness of the discretized bidomain-bath model using the finite element scheme. We derived a series of a priori estimates based on a general L^2-compactness criterion to prove the convergence of the chosen numerical schemes. For the convergence proof of the adjoint problem (because of the lack of the L^2-compactness), we use the discrete Sobolev embedding inequalities with general boundary conditions and a space-time L^1-compactness argument that mimics the compactness lemma due to S.N. Kruzhkov (this ingredient has an interest for various applications).

To support the numerical schemes used for the optimal control of bidomain-bath model, we demonstrated the numerical tests to achieve the successful cardiac defibrillation by utilizing the less total current. Moreover, we demonstrated the robustness of the Newton optimization algorithm for different finer mesh geometries and observed that the optimization algorithm converged superlinearly at all these finer meshes.

Acknowledgment. We would like to thank Prof. Karl Kunisch (University of Graz, Austria) for his support and suggestions, which helped us to considerably improve the manuscript.

REFERENCES

[1] B. Ainseba, M. Bendahmane, and R. Ruiz-Baier. Analysis of an optimal control problem for the tridomain model in cardiac electrophysiology. *Journal of Mathematical Analysis and Applications*, 388(1):231 – 247, 2012.

[2] B. Andreianov, M. Bendahmane, K. H. Karlsen, and C. Pierre. Convergence of discrete duality finite volume schemes for the cardiac bidomain model. *Networks and Heterogeneous Media*, 6(2):195–240, 2011.

[3] B. Andreianov, M. Bendahmane, A. Quarteroni, and R. Ruiz-Baier. Solvability analysis and numerical approximation of linearized cardiac electromechanics. *Mathematical Models and Methods in Applied Sciences*, 25(05):959–993, 2015.

[4] P. Bastian, M. Blatt, A. Dedner, C. Engwer, R. Klöfkorn, R. Kornhuber, M. Ohlberger, and O. Sander. A generic grid interface for parallel and adaptive scientific computing. Part II: implementation and tests in DUNE. *Computing*, 82(2):121–138, July 2008.

[5] M. Bendahmane and K. H. Karlsen. Analysis of a class of degenerate reaction-diffusion systems and the bidomain model of cardiac tissue. *Networks and Heterogeneous Media*, 1(1):185–218, 2006.

[6] M. Blatt. *A parallel algebraic multigrid method for elliptic problems with highly discontinuous coefficients*. PhD thesis, Ruprechts-Karls-Universität Heidelberg, 2010.

[7] Y. Bourgault, Y. Coudiére, and C. Pierre. Existence and uniqueness of the solution for the bidomain model used in cardiac electrophysiology. *Nonlinear Analysis: Real World Applications*, 10(1):458–482, 2009.

[8] A. J. Brandao, E. Fernandez-Cara, P. M. Magalhaes, and M. A. Rojas-Medar. Theoretical analysis and control results for the fitzhugh-nagumo equation. *Electronic Journal of Differential Equations (EJDE) [electronic only]*, 2008:Paper No. 164, 20 p., electronic only–Paper No. 164, 20 p., electronic only, 2008.

[9] H. Brezis. Analyse fonctionnelle, théorie et applications. *Masson, Paris*, 1983.

[10] E. Casas, C. Ryll, and F. Tröltzsch. Sparse optimal control of the schlögl and fitzhugh-nagumo systems. *Comput. Meth. in Appl. Math.*, 13(4):415–442, 2013.

[11] N. Chamakuri and K. Kunisch. Primal-dual active set strategy for large scale optimization of cardiac defibrillation. *submitted*, 2015.

[12] N. Chamakuri, K. Kunisch, and G. Plank. Numerical solution for optimal control of the reaction-diffusion equations in cardiac electrophysiology. *Computational Optimization and Applications*, 49:149–178, 2011. 10.1007/s10589-009-9280-3.

[13] N. Chamakuri, K. Kunisch, and G. Plank. Optimal control approach to termination of re-entry waves in cardiac electrophysiology. *Journal of Mathematical Biology*, pages 1–30, 2013. 10.1007/s00285-012-0557-2.

[14] N. Chamakuri, K. Kunisch, and G. Plank. PDE constrained optimization of electrical defibrillation in a 3D ventricular slice geometry. *International Journal for Numerical Methods in Biomedical Engineering*, 2015.

[15] R. Fitzhugh. Impulses and Physiological States in Theoretical Models of Nerve Membrane. *Biophysical Journal*, 1:445–466, July 1961.

[16] P. C. Franzonea and G. Savaré. Degenerate evolution systems modeling the cardiac electric field at micro- and macroscopic level. *Birkhäuser Verlag*, 50:49–78, 2006.

[17] C. S. Henriquez. Simulating the electrical behavior of cardiac tissue using the bidomain model. *Crit. Rev. Biomed. Eng.*, 21:1 77, 1993.

[18] D. A. Hooks, K. A. Tomlinson, S. G. Marsden, I. J. LeGrice, B. H. Smaill, A. J. Pullan, and P. J. Hunter. Cardiac microstructure: Implications for electrical propagation and defibrillation in the heart. *Circulation Research*, 91(4):331–338, 2002.

[19] S. N. Kruzhkov. Results on the nature of the continuity of solutions of parabolic equations, and certain applications thereof. *Mat. Zametki*, 6:97–108, 1969.

[20] K. Kunisch and M. Wagner. Optimal control of the bidomain system (III): Existence of minimizers and first-order optimality conditions. *ESAIM: Mathematical Modelling and Numerical Analysis*, 47:1077–1106, 7 2013.

[21] C. Mitchell and D. Schaeffer. A two-current model for the dynamics of cardiac membrane. *Bulletin of Mathematical Biology*, 65(5):767–793, 2003.

[22] R. Plonsey. Bioelectric sources arising in excitable fibers (ALZA lecture). *Ann Biomed Eng*, 16(6):519–46, 1988.

[23] B. J. Roth. Electrical conductivity values used with the bidomain model of cardiac tissue. *IEEE Trans Biomed Eng*, 44(4):326–328, Apr 1997.

[24] L. Tung. *A bi-domain model for describing ischemic myocardial DC potentials.* PhD thesis, MIT, Cambridge, MA, 1978.

[25] M. Veneroni. Reactiondiffusion systems for the macroscopic bidomain model of the cardiac electric field. *Nonlinear Analysis: Real World Applications*, 10(2):849 – 868, 2009.